Characterising European low renewable availability events in present and future climate model data

Meteorological Applications

RMetS Royal Meteorological Society

RESEARCH ARTICLE OPEN ACCESS

Characterising European Low Renewable Availability Events in Present and Future Climate Model Data

David J. Brayshaw[1] | Salim Poovadiyil[1] | Laura West Fischer[2] | Daniel B. Kirk-Davidoff[2]

[1]Department of Meteorology, University of Reading, Reading, Berkshire, UK | [2]EPRI, Palo Alto, California, USA

Correspondence: David J. Brayshaw (d.j.brayshaw@reading.ac.uk)

Received: 14 November 2025 | **Revised:** 7 May 2026 | **Accepted:** 12 May 2026

Keywords: climate model | climate projection | dunkelflaute | electricity | energy | power | reanalysis | renewables

ABSTRACT

Multi-day periods featuring low wind and solar generation ('Dunkelflaute', DF) are an increasing concern for European electricity systems. Understanding DF and how they may change is critical for assessing the risk of electricity supply shortfalls in power systems containing high levels of variable renewable generation. This study assesses the suitability of data from two versions of the EU's flagship Copernicus climate service (C3S-Energy and ECEM) for characterising DF events in the present-day, and uses these datasets to develop plausible scenarios of change under 2°C global warming. After controlling for issues of dataset quality, a broadly consistent picture of DF behaviour over the historic period (1980–2010) emerges. As expected, DF predominantly occurs in winter and responds coherently to the North Atlantic Oscillation (NAO) as the dominant large-scale mode of regional atmospheric variability. The continental-scale patterns of behaviour seen in the observationally based components of the datasets are well-replicated in the corresponding climate model-based data, but individual simulations can differ substantially at the scale of individual countries (these differences are found both within and between each dataset). The multi-model mean response to a 2°C global warming scenario in both ECEM and C3S-Energy suggests an increase in DF events ~5%–25% over much of the European domain (particularly the north and west). However, individual model responses exhibit very different patterns with one model suggesting a widespread ~5%–25% decrease in DF (i.e., a change of similar magnitude but opposing direction). Five distinct storylines of a 2°C global warming scenario are therefore proposed, providing a compromise between representing diversity of the individual responses while retaining a tractable set of outcomes. The ability to robustly project future DF behaviour (and future renewable energy climate more broadly) is severely limited by the small sample of climate projections typically available. Future analysis should therefore seek to consider a more extensive and comprehensive ensemble of climate simulations to develop greater confidence and understanding.

1 | Introduction

The share of renewable energy (wind and solar) in electric power production across major European countries reached 28% in 2024 and is on pace to exceed 40% by 2030 (Ember 2025). Since wind and solar energy generation are inherently weather-dependent, their output fluctuates over time. Recently, there has been a growing focus on the occurrence of prolonged periods of extremely low wind and solar power production, commonly referred to as 'dunkelflaute' (DF; Bloomfield et al. 2020; Drücke et al. 2021; Kaspar et al. 2019; Otero et al. 2022; van der Wiel, Bloomfield, et al. 2019; van der Wiel, Stoop, et al. 2019). These extended low-power events significantly reduce renewable electricity availability and strain the energy system, especially in regions with a high fraction of electrical generation from renewable sources. If such conditions coincide with periods of high demand, they can pose a risk of energy shortfalls. In recent years, several such events have been reported across different regions of Europe (Dawkins et al. 2020; Li et al. 2021; Wilczak et al. 2025).

Winter DF events are particularly important—especially in Northern Europe—where the demand for energy reaches its annual peak.

The European Network of Transmission System Operators for Electricity (ENTSO-E) has identified climate change as a critical factor influencing system adequacy and is seeking to develop methods to incorporate these risks into future electricity adequacy assessments (ENTSO 2020; Dubus et al. 2022). More broadly, an increasing number of datasets have been developed to fill data gaps and support the analysis of climate risk in renewable energy assessments. Many projects have utilised reanalysis-based datasets to generate wind and solar photovoltaic (PV) power time series, making them accessible to researchers and stakeholders at different spatial scales, including country-level ('NUTS0' in the EU's Nomenclature of Territorial Units for Statistics) and sub-country levels. Notable examples include EMHires (Gonzalez Aparicio et al. 2017), Renewables.ninja (Staffell and Pfenninger 2016), Restore (Kies et al. 2016) and datasets developed by the University of Reading (e.g., Bloomfield, Brayshaw, Gonzalez, and Charlton-Perez 2021). These datasets provide a crucial foundation for understanding past and present variability in renewable energy generation, offering insights into the impacts of extreme weather events like DF. Several studies have conducted intercomparison analyses to evaluate the reliability and consistency of these datasets (Kies et al. 2021; Moraes Jr et al. 2018).

Most of the available datasets are, however, intrinsically historical (i.e., backward looking) as they are derived primarily from meteorological reanalyses such as ERA5 and MERRA2. Forward looking datasets, in contrast, require future climate change projections and typically involve explicit use of outputs from complex numerical climate models (i.e., global climate models and/or earth system models—GCMs and ESMs—or downscaled weather variables from regional climate models—RCMs). The European Copernicus Climate Services (C3S) has produced an example of this type of energy-climate dataset, which includes daily or sub-daily wind and solar power time series, based on regional climate model output from the EURO-CORDEX project. The resulting dataset provides a suite of simulations using the IPCC's Representative Concentration Pathway (RCP) scenarios for a subset of EURO-CORDEX models. Multiple versions exist including the original C3S-ECEM prototype demonstrator (Troccoli et al. 2018) and the operational C3S-Energy service (Dubus et al. 2023) with newer versions of the latter continuing to be produced.

Several studies have established a strong link between periods of low renewable energy production and persistent high-pressure systems (atmospheric blocking) over Europe (Bloomfield, Brayshaw, Gonzalez, and Charlton-Perez 2021; Drücke et al. 2021; Mockert et al. 2023; van der Wiel, Stoop, et al. 2019). Studies have also confirmed a significant relationship between European blocking and different phases of the North Atlantic Oscillation (NAO; Davini et al. 2012; Feldstein 2003; Sung et al. 2011; Yao and Luo 2015). European blocking therefore influences the frequency and intensity of wind droughts, cloud cover and cold spells over Europe, and the characteristics of European blocking are in turn strongly affected by the large-scale atmospheric circulation. Accurately characterising and quantifying the characteristics of such weather-driven stress events, how they respond to climate variability, and how they change into the future is crucial for power grid operators to effectively balance supply and demand and ensure system reliability (Dawkins et al. 2020; Novacheck et al. 2021; Bloomfield 2025).

Although it is reasonable to expect that the data products from the various climate services for energy (such as C3S-Energy) have been subjected to internal quality assessment in terms of their aggregate properties, it is well understood that climate models tend to have biases in their representation of European blocking (typically misrepresenting their location, frequency and the persistence; Bacer et al. 2021; Davini and d'Andrea 2020; Woollings et al. 2018; Schiemann et al. 2020). Moreover, there is no clear consensus on how atmospheric blocking will change in the future with climate modelling studies often showing conflicting results: some suggesting a decrease in blocking events over the Euro-Atlantic region (Dunn-Sigouin and Son 2013; Matsueda and Endo 2017), others an increase (Mokhov et al. 2014), while others find no significant change (Masato et al. 2014). As such, while climate model derived data is potentially a powerful tool for energy scientists wishing to estimating the impact of climate change on DF, it is important to assess both how well existing energy-climate datasets accurately represent DF, and the extent to which their future projections of changes in DF are coherent and consistent.

This study therefore begins by assessing the extent to which the climate model-based simulations in two EU Copernicus climate service datasets, C3S-Energy service and its ECEM predecessor, provide a consistent foundation for understanding DF events in the historical period. Following this assessment, the extent to which DF events are projected to change in the future is investigated and a series of storylines (or scenarios) proposed to efficiently represent the associated uncertainty. Where possible, the analysis seeks to approach the problem as an energy user, focusing on the energy science implications, rather than seeking to understand the detailed physical meteorological drivers.

The remainder of this paper is structured as follows: Section 2 describes the data sources while Section 3 performs a basic analysis before defining a metric to identify DF events. Section 4 examines DF events in the historical period, comparing the GCM-based simulations against their corresponding reanalyses. Section 5 expands on this to develop a set of storylines describing projected changes in DF events under a future 2°C warming climate scenario. A concluding discussion is provided in Section 6.

2 | Data Sources

In the following section, the ECEM and C3S-Energy datasets are first described, including a brief evaluation of the 'historical climatological reference' within each dataset. Despite these historical climatological references being based on meteorological reanalysis products, there are marked differences between the two datasets with important implications for the identification of DF events. This is discussed in detail in Section 2.2.

2.1 | Energy-Climate Datasets

This paper focusses on evaluating the extent to which two leading energy-climate datasets reproduce and project changes in DF events impacting the European region. The two datasets share a common heritage and are freely available for public use via the Copernicus Climate Data Store (CDS) platform. The overall process by which these datasets are produced is illustrated in Figure 1.

European Climatic Energy Mixes (ECEM, Troccoli et al. 2018) provides nationally aggregated energy variables covering Europe at up to daily resolution. Indicators span both climate and energy properties including wind speed, global horizontal irradiance and temperature, as well as estimates of wind power, solar PV and demand. The ECEM data are derived from two sources of climate data. Historical reconstructions (1979–2016) are produced from a bias-adjusted version of the ERA-Interim reanalysis product for wind (Jones et al. 2017) and from the raw ERA-Interim dataset for solar. Climate projections are based on 6 different EURO-CORDEX model combinations (4 different GCMs producing 6 different global simulations downscaled by 6 different RCMs; see Bartók et al. 2019 for details on the selection methodology and Table S1 for a detailed list of those used here). Output covers 1979–2100 for each of the RCP4.5 and RCP8.5 climate scenarios though, for simplicity, only the RCP8.5 data are considered to create the 2°C global warming scenarios in this study.

COPERNICUS Climate Change Service for Energy (C3S-Energy or C3S-E; Dubus et al. 2023) is an operationalised update to the ECEM proof-of-concept demonstrator. Energy variables contained in the dataset span a similar range of climate and energy properties to ECEM, though many of them are provided at enhanced temporal resolution (3-hourly rather than daily). In contrast to ECEM, however, the newer ERA-5 reanalysis (Hersbach et al. 2020) is used to produce a reconstruction over the historic period (1979–2023). As in ECEM, EURO-CORDEX models are used as the basis of climate projections, with output recorded for the period 2005–2100 under scenarios RCP2.6, 4.5 and 8.5 (though again only RCP8.5 is considered in this study). In this case, 11 GCM-RCM combinations are available for use (6 different GCMs producing 8 different realisations, downscaled by 8 different RCMs; see Bartók et al. 2019 for details on the selection methodology and Table S1 for a detailed list of those used here). C3S-Energy continues to evolve as an operational service and most recently a version based on CMIP6 output was released (Copernicus 2024). This newer version is, however, excluded from the analysis in this paper as there is less than a decade of overlap between the observed historical period derived from reanalysis and the climate model projections.

Both ECEM and C3S-Energy use a similar two-step process to convert the climate data into energy variables (see Figure 1). First, the raw climate model output is bias-adjusted towards a reanalysis dataset (see also Section 2.2 for more detailed discussion) and then, secondly, the bias-adjusted meteorological variables are used to calculate renewable energy indicators using physically-based models (e.g., representative wind-power curves). A brief recap of the methodology for each of wind- and solar-power conversions is provided below. Further details for ECEM can be found in Bloomfield, Brayshaw, Troccoli, et al. (2021) (and the ECEM website, ECEM 2025, along with references therein) and relevant documentation on the COPERNICUS Climate Data Store (Copernicus 2025; Trocolli et al. 2024) for C3S-Energy.

- For wind power: at each grid-point the 10 m winds are extrapolated to 100 m; converted to capacity factor using a representative power curve (for ECEM only onshore locations are considered, for C3S-Energy a different power curve is used for offshore and onshore); then spatially averaged to produce a single national capacity factor assuming a uniform distribution.
- For solar PV: at each grid-point the irradiance, temperature and zenith angle are passed through an empirical power curve to produce a capacity factor, which is then again spatially averaged to produce a single national capacity factor assuming a uniform distribution.

For both datasets, analysis in this publication is performed using nationally-aggregated daily data for wind- and solar PV capacity factors over a common period of 1980–2010. The data are downloaded directly from CDS in the case of C3S-Energy. For ECEM, the relevant data can readily be downloaded from the ECEM website. To facilitate bulk analysis in this paper a copy of the dataset was in this case obtained directly from the ECEM developers. Throughout the paper, the data sources used are indicated by unambiguous two-or-three-word combinations linking the project and the model used. For example, (a) C3S-ERA5 and (b) ECEM-CNRM-ALA are used to denote data from (a) the C3S-Energy dataset derived from the ERA5 reanalysis and (b) the ECEM dataset CNRM GCM downscaled with ALADIN RCM respectively.

A key point to note is that the energy-data derived from climate models in both C3S-Energy and ECEM originates from a very

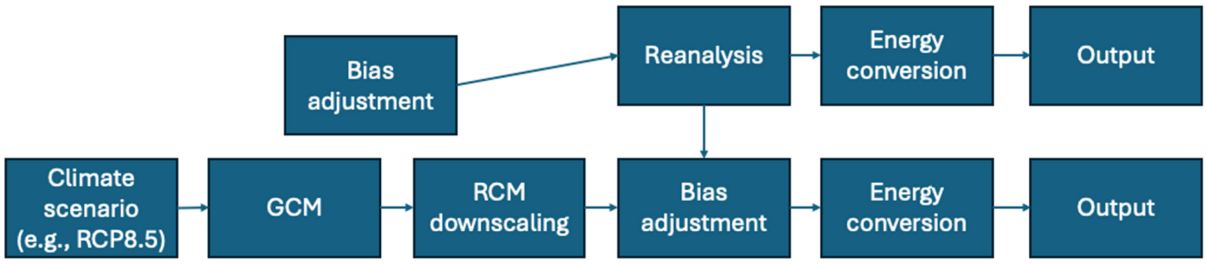

FIGURE 1 | Schematic diagram of the process through which ECEM and C3S-Energy datasets are created.

similar set of simulations: that is, a subset of EURO-CORDEX RCMs applied to CMIP5 global climate model output, selected using the method of Bartók et al. (2019). Where energy-variables derived from same GCM-RCM model pair appear in both C3S-Energy and ECEM, the differences between the output can therefore be attributed to the bias-adjustments and energy-conversion methods, rather than differences in the underlying climate data (it is particularly emphasised also that C3S-Energy includes offshore and onshore wind, while ECEM considers onshore only). Similarly, where two different RCMs downscale the same parent GCM simulation within C3S-Energy, the differences can usually be ascribed to the choice of RCM (e.g., C3S_MPI_XXX and C3S_HAD_XXX). It is, however, noted that in the case of the EC-EARTH (used in both C3S-Energy and ECEM) the multiple RCM downscalings corresponding to different realisations of the parent GCM (r1i1pi, r3i1p1 and r12i1pi). Differences between the EC-EARTH based simulations are therefore potentially caused by a mixture of both internal variability (i.e., the initial conditions used to start the EC-EARTH simulation) as well as RCM selection. Readers are referred to the table of the simulations and model combinations provided in Table S1 for details.

As will be discussed in Section 2.2, in the case of ECEM, a third dataset was required to support the evaluation of wind-power capacity factors in the historic period. This additional dataset provides daily wind-power capacity factors based on the WFDEI reanalysis (a different bias-adjusted version of the ERA-Interim reanalysis; Weedon et al. 2014). This data were sourced from https://esgf-node.ipsl.upmc.fr/projects/esgf-ipsl. It is noted, however, that this is not provided on the ECEM platform itself. To make this contrast clear, the original reanalysis-based data from the ECEM website is referred to as ECEM-ERAInt (both for solar and for wind), while this additional reanalysis-based data is referred to as ECEM-WFDEI.

2.2 | Historical Climatological Reference

In order to define a specific metric to characterise DF the gross properties of the C3S-Energy and ECEM datasets are first examined as a baseline. It is emphasised that this examination is not intended to provide a detailed comparison between C3S-Energy and ECEM, nor an evaluation of the accuracy of their respective weather-to-energy conversion models in absolute terms. As will be discussed, however, there are significant inconsistencies in the representation of renewable capacity factors both between and within each dataset. The analysis in this section is therefore provided in order to motivate the choice of DF metric as set out subsequently in Section 3.

Figure 2 presents the 1980–2010 climatology of wind and solar capacity factors for Germany based on reanalysis datasets and climate model derived estimates from ECEM and C3S-Energy (Germany is selected as a representative example, other countries can be found in the Figures S1 and S2). For context, the average annual capacity factors for Germany in 2024 were around 20% for onshore wind, 32% for offshore wind (87% of total installed wind capacity was onshore) and 8% for solar PV (Bundesministerium für Wirtschaft und Energie 2025).

For wind capacity factors (Figure 2a), both ECEM and C3S-Energy exhibit a well-defined seasonal cycle in their respective reanalysis estimates (ECEM-ERAInt and C3S-ERA5, dashed and solid black lines, respectively), with higher values in winter and lower values in summer. Moreover, in both datasets, the climate-model equivalents show a qualitatively similar annual cycle (coloured lines). There are, however, clear differences both between ECEM and C3S-Energy as well as inconsistencies within each dataset.

Firstly, there is a substantial difference in the wind-power capacity factors recorded in the two datasets, with C3S-ERA5 typically between 0.1 to 0.2 CF higher than ECEM-ERAInt: that is, time-averaged capacity factors can be markedly different between these two products. This is somewhat consistent with the wind-power modelling assumptions made in the two datasets (e.g., different power curves and, for some countries, ECEM considers only onshore wind whereas C3S-Energy includes offshore regions that typically exhibit much higher CF values, Drew et al. 2015). Moreover, within the C3S-Energy dataset, the climate models are closely consistent with each other (the solid coloured lines are near-identical), suggesting a strong level of bias-adjustment has been performed towards a common reference climate state. However, the climate models (coloured solid lines) are markedly different from their corresponding reanalysis (C3S-ERA5, solid black line). A similar problem is found in the corresponding ECEM simulations, whereby the ECEM-ERAInt wind-power capacity factor (dashed black line) has a somewhat different mean annual cycle to the climate models (which are nevertheless remarkably consistent between themselves, indicated by the coloured dashed lines). In the case of ECEM, this appears to be caused by the climate models being adjusted towards the ECEM-WFDEI baseline (dot-dash black line), although ECEM-WFDEI is not provided on the ECEM website. We are not aware of a corresponding alternative reanalysis for C3S-Energy, but it is noted that the issue identified here is not restricted to particular locations: similar discrepancies are found across other country wind-power capacity factors (see Figure S1).

For solar capacity factors (Figure 2b), the seasonal cycle of solar power capacity factor is generally well captured across datasets on a qualitative level. Again, however, there are noticeable differences between the datasets with C3S-Energy reanalysis (C3S-ERA5) typically recording higher solar PV capacity factors than ECEM (ECEM-ERAInt, ~0.05 CF in this particular country but a qualitatively similar picture emerges across many countries, see Figure S2). Within the ECEM dataset the climate models (coloured dashed lines) give an almost identical annual cycle of solar PV capacity factors when compared against their corresponding reanalysis (ECEM-ERAInt, black dashed line). By contrast, within C3S-Energy, most of the climate model derived data tend to exhibit a slightly lower solar capacity factors in winter compared to its own reanalysis C3S-ERA5 (compare the solid red, brown and light green lines for C3S-CNRM-ALA, C3S-HAD-REGCM and C3S-ECE-HIR with the C3S-ERA5 solid black line), indicating a systematic underestimation of solar PV potential compared to the relevant reanalysis. Moreover, some of the C3S-Energy climate models (e.g., C3S-HAD-RAC, C3S-MPI-CCL, CRS-ECE-RAC and C3S-NOR-HIR in light yellow, light pink, mid-green and dark blue solid lines) appear to be bias adjusted towards a different climatology (similar to

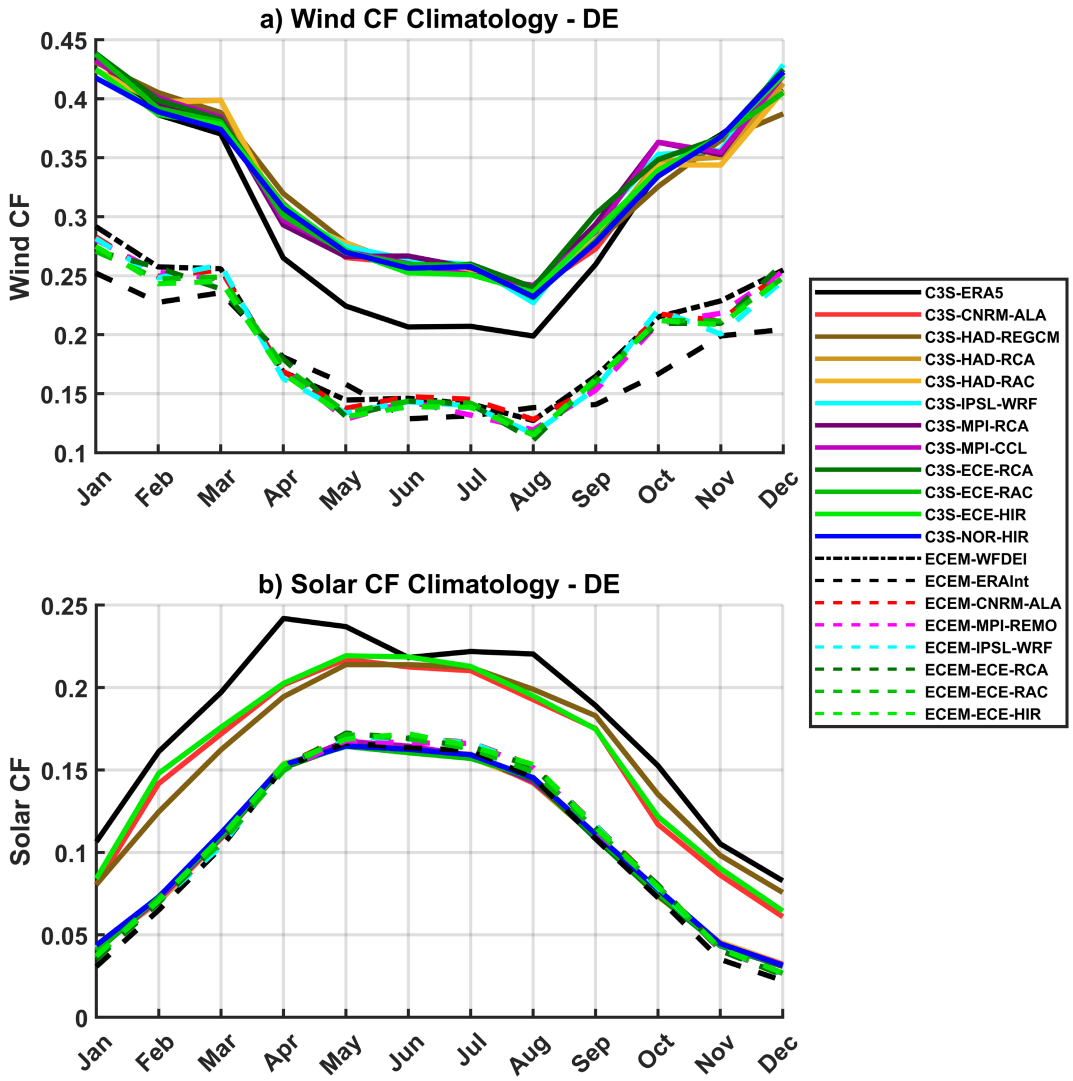

FIGURE 2 | Comparison of mean annual cycle in ECEM and C3S-Energy datasets (1980–2010) for Germany: (a) wind capacity factor, (b) solar capacity factor. Black lines relate to reanalysis based estimates, coloured lines to climate-model based estimates. Solid lines related to C3S-Energy, dashed lines to ECEM.

ECEM-ERAInt rather than C3S-ERA5) creating inconsistency within the C3S-Energy dataset.

The inconsistencies both between and within the datasets discussed above clearly have important implications for assessments reliant on absolute capacity factor values (e.g., estimating mean capacity factor or counts of days where capacity factor falls below a particular threshold). This suggests that although the datasets may provide useful climatological information, caution must be exercised when using them for energy modelling—that is, the values recorded in ECEM or C3S-Energy should not be used in energy-modelling without first assessing their accuracy and re-calibrating if needed.

3 | Dunkelflaute Definition and Assessment of the Observed Meteorological Period

Prior to assessing the representation of DF in the climate-model derived data, this section defines an objective metric representing DF events and compares how these events are represented in the 'reanalysis' products within ECEM and C3S-Energy.

There is no standardised method for identifying DF events (or renewable resource droughts in general), with the characterisation of renewable energy droughts—including their frequency, duration and severity—being highly sensitive to the chosen definition (Kittel and Schill 2024). In broad terms, two 'types' of DF definitions can be identified at daily timescales defined by either: (a) absolute capacity factor thresholds (e.g., capacity factors below, say, 0.2; Leahy and McKeogh 2013; Patlakas et al. 2017; Ohlendorf and Schill 2020) or (b) quantile thresholds relative to some reference climatology (e.g., capacity factors below, say, the 20th percentile of the local capacity factor distribution; Cannon et al. 2015).

Due to the gross differences between the ECEM and C3SE datasets discussed in Section 2.2, a quantile-based threshold (i.e., the 30th percentile of the relevant distribution) is adopted to identify low renewable resource events. The number of events identified

TABLE 1 | Climatological annual rate of low wind, solar and low wind-and-solar CF in the ECEM and C3S-Energy reanalyses (1980–2010).

	Low wind CF (below 30th percentile)			Low solar PV CF (below 30th percentile)		Combined low wind and solar CF (both below 30th percentile)		
Days/year	C3SE-ERA5	ECEM-ERAInt	ECEM-WFDEI	C3SE-ERA5	ECEM-ERAInt	C3SE-ERA5	ECEM-ERAInt	ECEM-WFDEI
Bulgaria	110	109	105	110	109	19	28	21
France	110	109	109	110	109	15	19	16
Germany	110	109	110	110	109	18	23	20
Spain	110	109	108	110	108	16	29	20
Sweden	110	108	107	110	109	18	30	21
UK	110	109	109	110	109	19	25	20

Note: 'Low' conditions are defined as below the 30th percentile of each property.

are shown in Table 1. By construction, the number of low wind-power and low solar PV days per year is similar across the datasets (i.e., approximately 30% of days, subject to minor differences associated with the precise definition of the climatology and intercomparison period). This choice therefore has the advantages that it: identifies genuine compound events (i.e., both wind- and solar-production has to be well below their 'average' output level rather than merely events where low-wind or low-solar occurs individually); facilitates inter-dataset comparison by avoiding the gross mismatch between their absolute values; and avoids the need to specify a given 'future' installed generation capacity scenario (as these are highly uncertain). It is, however, noted that there remain differences in the count of joint low-wind-low-solar power events, with C3S-ERA5 typically producing fewer such days than ECEM-WFDEI (by ~5%–10%) and ECEM-ERAInt (by ~50%). This indicates that subtle differences either between the meteorological conditions recorded in the reanalyses (e.g., the correlation between low wind and low solar conditions) or in the conversion methodologies (e.g., use of different wind-power curves) are producing significant differences in the characterisation of low renewable resource conditions. Interested readers can also find an equivalent analysis using an absolute CF-threshold method (CF < 0.2) in Table S2 (using an absolute CF method leads to much more marked difference between DF characteristics in ECEM and C3SE due to the gross differences in their recorded capacity factors as discussed in Section 2.2).

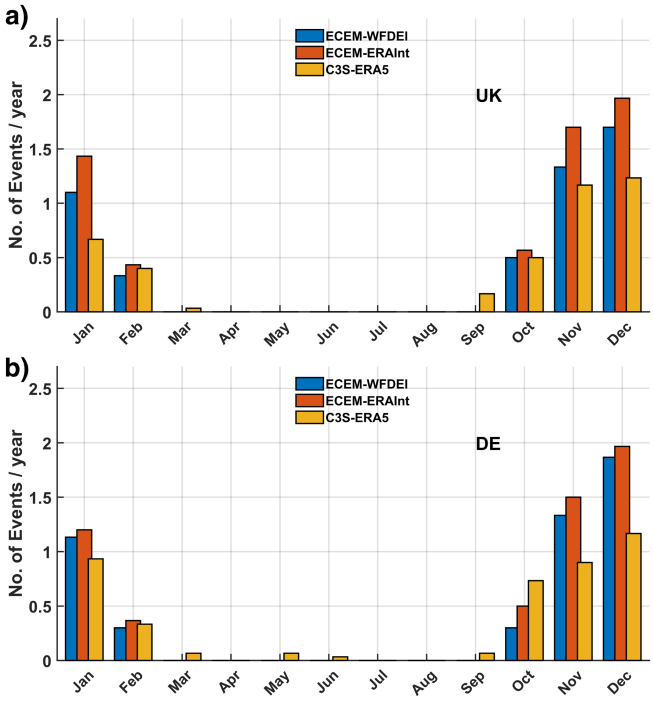

FIGURE 3 | Annual cycle of DF event (2 days or more) frequency for the historical period (1980–2010) in reanalysis datasets associated with ECEM and C3S-Energy for (a) the UK and (b) Germany.

For each country a 'DF day' is said to occur when both the daily-mean windCF and solarCF fall below the 30th percentile of their dataset-dependent climatological distribution (taken across all days of the year). A 'DF event' is defined as a period for which two or more consecutive days experience such conditions.

The resulting annual cycle of DF events for the UK and Germany is shown in Figure 3, confirming a strong seasonal cycle (peaking between October and February and almost absent over the summer months May to August) and broadly consistent behaviour is found across Europe (see Figure S3 for further examples). The seasonal pattern is consistent with the expected variability in wind and solar resources, where reduced wind speeds and lower solar insolation in winter contribute to an increased risk of extreme low renewable power production, though the relative contributions from wind and solar in generating DF events are likely to depend on geographical location (e.g., differing seasonal cycles of insolation of wind climate). The count-frequency of the C3S-ERA5 estimates aligns qualitatively with previous studies: for example Kaspar et al. 2019 adopted a definition of DF of a combined capacity factor CF < 0.1 persisting for 48 h (assuming equal installed capacity) finding an annual frequency of just over 4 DF events per year on average in Germany (see their Figure 6). ECEM-WFDEI and ECEM-ERAInt datasets exhibit a similar but slightly higher number of DF events compared to C3S-ERA5 (4.85 year^{-1} for ECEM-WFDEI vs. 4.2 year^{-1} for C3S-ERA5).

The geographical distribution of DF events (and comparison between the datasets) is shown in Figure 4, emphasising that

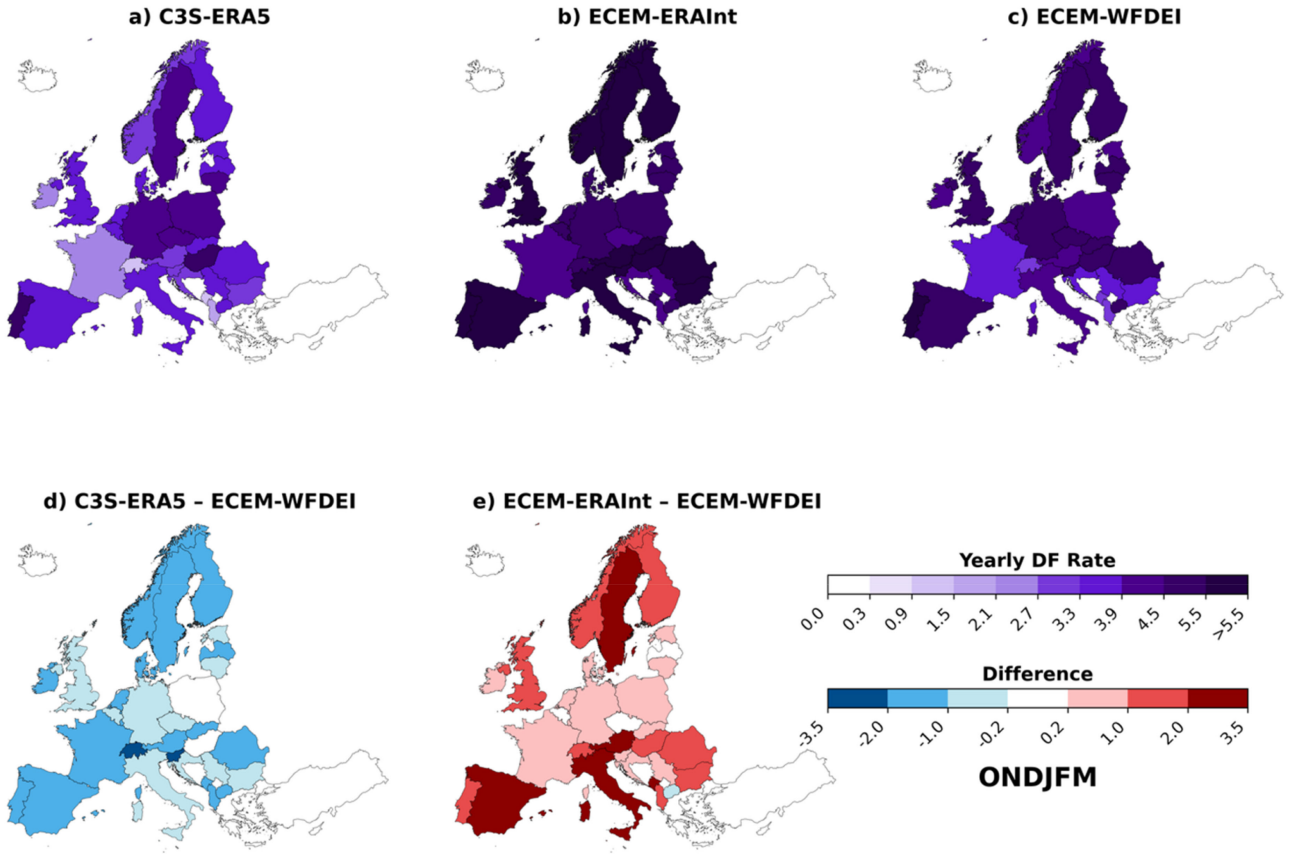

FIGURE 4 | Mean DF event frequency for the extended winter (ONDJFM, 1980–2010) in: (a) C3S-ERA5, (b) ECEM-ERAInt and (c) ECEM-WFDEI. Also shown are differences (d) C3S-ERA5 minus ECEM-WFDEI and (e) ECEM-ERAInt minus ECEM-WFDEI.

the differences in DF event frequency are reasonably consistent across the European domain (Panels a–c), as are the differences between the datasets (Panels d and e).

A key point to note, however, is that the absolute number of DF days or events will depend strongly on the thresholds chosen to define their occurrence. In particular, much of the difference between the winter-time DF events recorded in C3SE-ERA5 and ECEM-WFDEI is likely to be associated with differences in the representation of summer wind-climate in the two datasets (C3SE-ERA5 has climatologically lower windCF in summer—see Figures 2 and S1 for other example countries—thus suppressing the annual 30th windCF percentile threshold and reducing the likelihood of DF occurance in winter).

4 | Simulated Dunkelflaute in the Historical Period

This section evaluates the representation of DF events in the ECEM and C3S-Energy climate model datasets over the historical period (1980–2010). The analysis focuses on three key aspects: the frequency of DF events, their duration and their connection to large-scale atmospheric circulation patterns. It is noted that, henceforth, the ECEM-WFDEI reanalysis is used as a reference for the ECEM climate models (rather than the ECEM-ERAInt data provided by the ECEM website). ECEM-WFDEI is selected because, as discussed in Section 2.2, ECEM-WFDEI provides a closer match to the bias-adjustment applied to the ECEM climate models. The analysis is also restricted to the extended winter season (October through to March) as the core season for DF events.

It is also noted that, throughout the subsequent analysis, model-relative thresholds are used in determining DF-days (i.e., a DF day is declared when both wind and solar CF drop below the 30th percentile derived from each individual model's own climatology). The impact of deficiencies in the bias adjustment of the models towards their respective reanalyses (see Section 2.2) should therefore be somewhat reduced though, as noted in Sections 2.2 and 3, the exact characteristics of DF behaviour is highly sensitive to the metrics and thresholds used to identify them.

4.1 | Frequency of DF Events

Figure 5 illustrates the overall DF event frequencies across Europe for the individual models in each dataset (Panels e–u) and as a multi-model average (Panels b and d), comparing each against their own observed historical reanalysis climatology (i.e., C3S-ERA5 or ECEM-WFDEI, Panels a and c).

Examining the multi-model mean (Figure 5b,d) suggests that, on average, the ECEM climate models typically have smaller biases (less than 5%–25%) than their C3S counterparts (up to 50%–100%) when each is compared to their own reference reanalysis dataset. Moreover, while the ECEM multi-model mean presents a spatially mixed pattern (i.e., over- and under-estimates of DF events in different regions), the C3S multi-model mean tends to overestimate

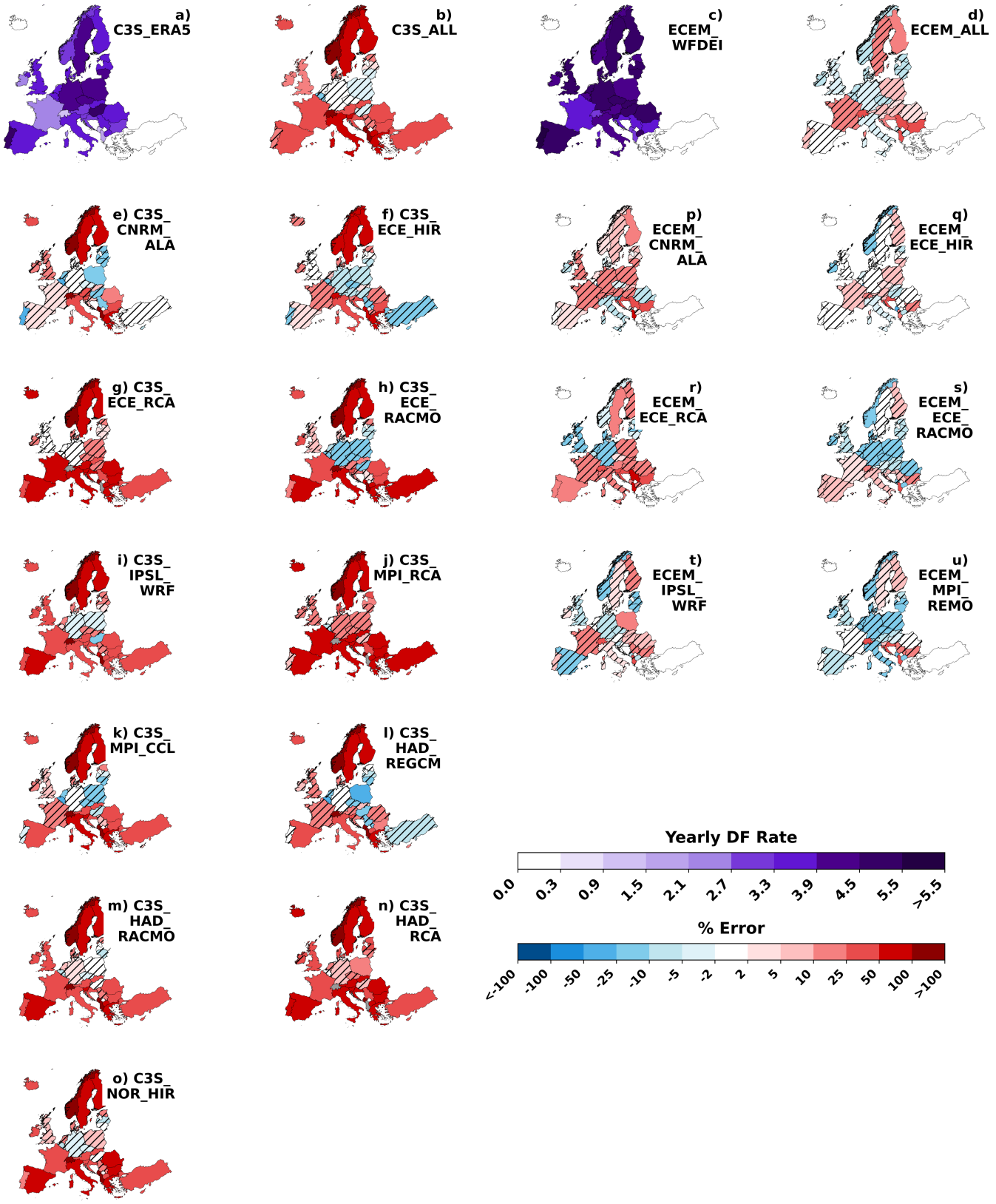

FIGURE 5 | Spatial distribution of DF event rate during extended winter (ONDJFM) in the historic period 1980–2010. (a) and (c) show the C3S-ERA5 and ECEM-WFDEI DF event rates reproduced from Figure 4. (b) and (d), respectively show the multi-model mean difference between the C3S-Energy and ECEM models against their appropriate reanalysis climatology. (e–o) show corresponding differences for individual C3S-Energy climate models. (p–u) are similar for the individual ECEM climate models. Plots (b), (d) and (e–u) are expressed as fractional differences from the relevant reanalysis on a country-by-country basis. Hatching denotes areas for which does not pass a Wilcoxon signed rank test does not pass with 90% confidence.

DF events in almost all countries but especially in the north/northwest (UK, Ireland, Scandinavia) and south (countries immediately around the Mediterranean's northern coastline).

In C3S-Energy, many of these differences are statistically significant at the 90% level (as indicated by the lack of hatching in Panel b).

Examination of the individual models within each dataset (Figure 5 Panels e–o for C3S-Energy and p–u for ECEM) reveals a similar overall pattern of behaviour to the multi-model mean. For ECEM, there are few countries where statistically significant differences are found. By contrast, most models in C3S-Energy exhibit statistically significant biases with respect to the C3S-ERA5 observed historical climatology over much of Europe, typically overestimating strongly in north/northwestern Europe and northern Mediterranean, while overestimating less strongly (or even slightly underestimating) in the east at central latitudes. While each C3S-Energy model seems to broadly follow this basic meridional tripole pattern (i.e., over-under-over estimates from north to south over the region), the C3S_ECE_RCA, C3S_MPI_RCA and C3S_HAD_RCA seem to have particularly strong positive biases while C3S-CNRM-ALA, C3S_ECE_HIR and C3S_HAD_REGCM are more evenly split (positive–negative–positive).

Taken across both C3S-Energy and ECEM there is perhaps some evidence that the RCA RCM is associated with a positive bias (each of ECEM_ECE_RCA, C3S_ECE_RCA, C3S_MPI_RCA and C3S_HAD_RCA tends to exhibit more DF events than their corresponding reanalysis equivalent). It is, however, extremely difficult to make strong statements about which GCMs, RCMs and GCM-realisations are associated with particular behaviour due to the ad-hoc construction of the model ensemble.

4.2 | Duration of DF Events

Figure 6 shows the extent to which the climate model simulations in ECEM and C3S-Energy correctly represent the extent of DF conditions across Europe for different durations. In each case, the climate models are compared to the corresponding reanalysis associated with the dataset. For convenience, a selection of six countries is discussed as 'typical' representative examples below. It is, however, noted that some countries can differ markedly from this broad assessment (including much larger differences between model and reanalysis estimates; see Figure S4), and careful case-by-case assessment is recommended when using individual country-level values.

For both shorter-duration events (2–3 days) and long-duration (4–5 days), the ECEM models exhibit a reasonable level of performance. Though the error magnitudes are large (up to 25% and ~50% respectively for the countries selected, Figure 6b,d), there is little systematic bias and using the 90% confidence interval as a qualitative indicator of uncertainty in these estimates suggests these differences are small. In general, performance is quite consistent across the various ECEM climate models, with differences between the models being less than the difference between the model and the corresponding reanalysis.

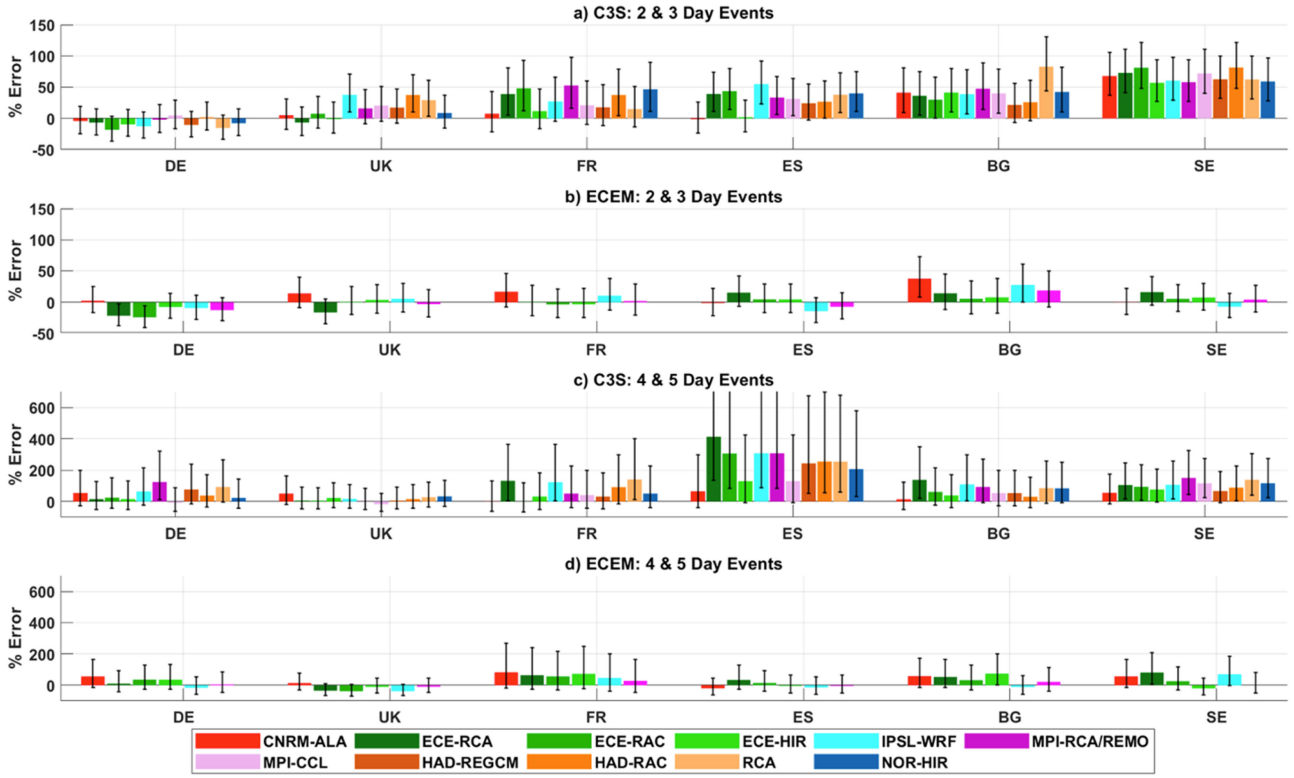

FIGURE 6 | Errors in DF event rates by duration for selected countries for extended winter (ONDJFM). (a) and (b) 2–3 day events in C3S-Energy and ECEM, respectively. (c) and (d) 4–5 day events. Errors are expressed as fractions of the country-specific DF event rate from the appropriate reanalysis (C3S-ERA5 or ECEM-WFDEI). The marked uncertainty ranges represent the 90% bootstrap confidence interval.

C3S-Energy, however, typically overestimates the rate of DF events by around 25%–50% (for 2–3 day events, Figure 6a) and 100%–200% (for 4–5 day events, Figure 6c). The cause of this larger discrepancy against their reanalysis (compared to the equivalent in ECEM) is unclear, particularly in cases where the same GCM-RCM pair is available in both cases (e.g., the simulations using CNRM_ALA, ECE_RCA, ECE_RAC, ECE_HIR, IPSL_WRF exist in both datasets).

Overall, the results suggest that ECEM models offer a more credible representation of DF events (compared to their own reanalysis), whereas C3S models show larger discrepancies compared to their own reanalysis. It is, however, important to emphasise that this result is likely sensitive to the choice of metrics used to identify DF. In particular, the use of the annual 30th percentile is likely to be associated with the C3S-Energy climate models overestimating DF compared to C3S-ERA5 due to their higher average windCF in summer (i.e., increasing the annual 30th windCF percentile and thus potentially making DF more prevalent in winter). The differences between the datasets nevertheless emphasise the need for greater consistency across energy climate service products when providing data derived from both climate model and reanalysis output.

4.3 | Large Scale Atmospheric Drivers of Dunkelflaute Rates

As discussed in Section 1, the wintertime North Atlantic Oscillation (NAO) plays a crucial role in shaping wind conditions across Europe, particularly influencing the occurrence of DF events. Here, the NAO index is calculated as the difference in extended winter (ONDJFM) mean sea-level pressure between the Azores (28°–20°W, 36°–40° N) and Iceland (25°–16°W, 63°–70°N). The resulting timeseries is normalised against the 1980–2010 period (following Smith et al. 2020) to have unit variance and zero mean. As the information to calculate the NAO is not available directly from either ECEM or C3S-Energy, surface level pressure data is downloaded from the corresponding parent GCM (see Figure 1 and Table S1) from the Copernicus Climate Data Store (Copernicus 2018). Positive states are defined as seasons where NAO >0.5 and negative where NAO <-0.5. Note that C3S_ECE_HIR and ECEM_ECE_HIR are excluded from the subsequent analysis (and greyed-out in the corresponding figures) as the required sea level pressure data from the parent GCM simulation was not available.

As a preliminary step to assessing the impact of NAO on DF events, Figures 7 and 8 show the impact of the winter NAO on mean wind and solar CF over Europe. For wind CF (Figure 7), there is a clear meridional dipole pattern such that, for positive NAO, wind is enhanced over much of northern Europe and decreased over southern Europe, consistent with previous studies (e.g., Brayshaw et al. 2009; Lledó et al. 2022). This pattern is found in both reanalysis-based datasets (i.e., C3S-ERA5 and ECEM-WFDEI, Panels a and c) and is broadly reproduced by each of the individual models (as shown in the multi-model average in Panels b and d). There are, however, notable inter-model differences suggesting that the reanalysis 'NAO response pattern' is not precisely reproduced. For example, the NAO response is rather stronger in the magnitude and extent of the increase in the north in, for example, C3S_IPSL_WRF and C3S_HAD_RACMO whereas the southern decrease is more dominant and extensive in C3S_CNRM_ALA and ECEM_MPI_REMO. This indicates that differences in spatial NAO structure between models may have important impacts at national level.

Figure 8 shows that the impact of the NAO on solar CF has a spatially similar NAO response pattern but the effect is weaker in magnitude and with the opposite sense (i.e., a meridional dipole with positive NAO is associated with reduced solar in the north, increased in the south). This is seen in both the reanalysis datasets (Panels a and c) and the multi-model average (Panels b and d), confirming a broad pattern consistent with previous studies (e.g., Pozo-Vázquez et al. 2004; Lledó et al. 2022). However, as with wind CF, there are potentially important differences between the modelled datasets: for example, C3S_IPSL_WRF shows a positive relationship between solar CF and NAO over some area of Scandinavia and especially Sweden which is not found in any other models (or indeed the ECEM_IPSL_WRF equivalent which uses exactly the same GCM-RCM data; see Panels i and t).

Focussing on DF events more specifically, Figure 9 shows the fractional change in DF events associated with NAO state. Both reanalysis-based estimates (C3S-ERA5 and ECEM-WFDEI, Panels a and c) show a clear dipole like-behaviour, with DF events being more frequent in northern and eastern Europe under NAO-negative and more frequent in southern and eastern Europe under NAO-positive. Though the precise details differ between the two reanalyses (e.g., for Ireland and France), the broad pattern is both consistent between the datasets and with previous studies (NAO-negative tends to be associated with increased blocking in northern Europe, and NAO-positive similarly for southern Europe, e.g., Yao and Luo 2015). The overall sense of the dipole (i.e., fewer DF events in the north under NAO positive) suggest that this reflect the NAO-impact on wind CF rather than the solar CF (compare Figure 9 vs. Figures 7 and 8 focussing on Panels a and c in each case). This is, however, not necessarily uniform across the whole domain (e.g., for the south east and especially Turkey the NAO–DF relationship is more consistent with the NAO–solarCF relationship).

In terms of the climate model response of DF events to NAO, the multi-model average in each dataset (Figure 9b,d) broadly resembles the dipole pattern of their corresponding reanalyses (Figure 9a,c). There are, however, noticable differences at the individual country level—for example, the impact of the NAO on both France and Germany reverses sign in C3S-Energy and ECEM respectively—and, overall, both the C3S-Energy and ECEM multi-model responses appear to show the lower part of the dipole (the red area in Panels b and d) extending further north and east into Europe compared to their equivalent reanalyses (the red areas in Panels a and c). As expected, the differences in the NAO responses are exacerbated in the individual model runs (Figure 9e–u). Most models do correctly capture the 'sense' of the meridional dipole seen in the reanalyses (i.e., consistent with producing fewer DF events in the north under NAO positive), but there are wide variations in the exact nature of this pattern: for example, C3S_IPSL_WRF and ECEM_IPSL_WRF show most of the region having fewer DF events under NAO

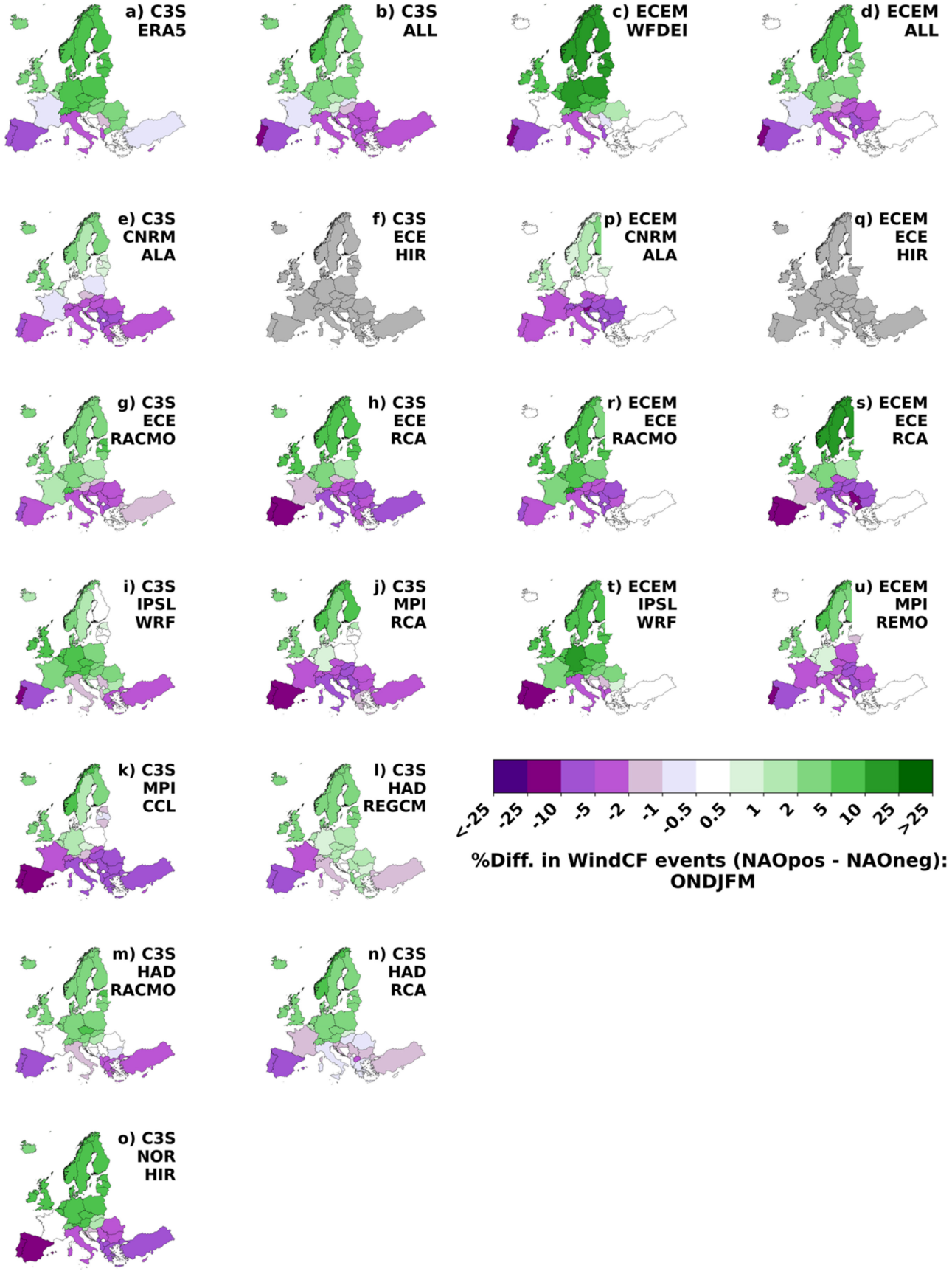

FIGURE 7 | Legend on next page.

FIGURE 7 | The impact of NAO state on mean wind CF during extended winter (ONDJFM) in the historic period 1980–2010 (NAO positive minus NAO negative expressed as a fractional percentage of the all-NAO-state-average). (a) and (c) show the C3S-ERA5 and ECEM-WFDEI response to NAO respectively. (b) and (d) show the C3S-Energy and ECEM multi-model mean response to NAO respectively. (e–o) show corresponding NAO response for individual C3S-Energy climate models. (p–u) show similar responses for the individual ECEM climate models. Plots (b), (d) and (e–u) are expressed as fractional differences from the relevant reanalysis or model's mean wind CF on a country-by-country basis.

positive whereas C3S_CNRM_ALA, ECEM_CNRM_ALA and to a lesser extent C3S_MPI_CCL and C3S_HAD_REGCM suggest the bulk of Europe has more frequent DF events (compare Figure 9i,t with Figure 9e,k,l,p). Again, due to the relatively small and ad-hoc construction of the climate model ensemble it is difficult to confidently discern whether any of these differences in response can be ascribed to particular GCMs, RCMs or simple internal variability.

In summary, the NAO's influence has—on average—somewhat opposing influences over much of Europe's renewables with more wind, less solar and fewer DF events in the north but less wind, more solar and more DF events in the south under positive NAO. This behaviour is broadly consistent in the ECEM and C3S reanalyses (ECEM-WFDEI and C3S-ERA5) and in the climate models in each archive. There are, however, differences between the NAO responses produced by the individual models (both spatially and in magnitude) which could have significant impact when considering either national-scale variations in renewable resource or the need for transmission and storage at national or continental level to balance climate variability at timescales from days to years. It is emphasised, however, that the sample sizes available to this analysis limit the extent to which the causes of these differences can be identified and as to whether they are associated with sampling uncertainty (i.e., the internal variability of the climate model) or genuine differences in climate model performance (i.e., some models producing more 'realistic' NAO signatures than others).

5 | Projected Changes in Dunkelflaute

As a first step in assessing future changes in DF events, a 2°C global warming level is assumed (IPCC 2023). A 30-year window is identified in each of the parent climate model simulations, centred on the date at which the global-mean surface air temperature first exceeds 2°C above from the model's own 1980–2010 climate. This limits the impact of individual GCMs having different global climate sensitivities (i.e., some GCMs warming faster than others in response to increased atmospheric greenhouse gas emissions). Figure 10 illustrates the process and the precise periods selected are listed in Table 2. In all cases the period lies in the mid 21st century but occurs substantially earlier in some models (~2029–2059 in HadGEM) and later in others (~2048–2078 in NorESM1).

Figure 11 shows the resulting scenarios aggregated over all the C3S-Energy (Panels a1–a4) and ECEM (Panels d1–d4) datasets. The subset of GCM-RCM simulations that appear in both datasets are shown in Panels b1–b4 (for C3S-Energy) and c1–c4 (for ECEM).

Consider first the changes in the extended winter average renewable capacity factors. There is limited evidence for strong or widespread changes in wind CF (Figure 11a1,b1,c1,d1), though the full set of C3S-Energy models (Panel a1) suggest some reduction of wind CF over the countries along the northern Mediterranean coast (especially Italy and Iberia, ~2%–5%) and weaker reductions in the west (particularly Norway and UK). There is also some evidence for slight increases in wind CF in the centre-east (e.g., Bulgaria, Romania and Hungary), though these changes are not significant. For context, typical interannual variability in the region corresponds to a ~10%–25% variation (corresponds to1 standard deviation, see Figure S5). A qualitatively similar pattern emerges from ECEM (Figure 11d1) and when only the subset of common models is considered from each dataset (Figure 11b1,c1). For solar CF, the pattern of change is more coherent with significant reductions particularly over the northern part of the region (~2%–5% decrease in both ECEM and C3S-Energy but more pronounced in ECEM, Figure 11a2–d2). For context, typical interannual variability in the region corresponds to a ~5%–10% variation (corresponds to1 standard deviation, see Figure S6).

In contrast to the modest changes in average wind and solar CF, the full set of C3S-Energy models suggest quite a marked and extensive increase of ~5%–25% in the number of DF days (Figure 11c1) and DF events (Figure 11d1), particularly in northern Europe. The stronger change in DF days or events (compared to wind or solar CF values) reflects the relatively strong variability in DF events (interannual variability of ~25%–50% in DF events compared to weaker variations for wind and solar CF; see Figures S6 and S7 and compare with Figures S4 and S5). This pattern is somewhat reproduced in ECEM (Figure 11, Panels d3 and d4) though, for ECEM, the models suggest a weak decrease in DF in the southern and eastern regions (e.g., Hungary). The differences between the two datasets are reduced when the multi-model average is restricted to only the common GCM-RCM simulations used in the two datasets (compare Figure 11, Panels b3 and b4 with Panels c3 and c4). This suggests that a large part—but not all—of the differences between the multi-model averages using the full C3S-Energy and ECEM datasets are associated with the GCM-RCM sample, rather than the specifics of the bias adjustment and energy-conversion processing.

This suggests that the 'result' of the multi-model-average is likely very sensitive to the composition of the underlying climate model ensemble used. This in turn implies that, if just a few GCM-RCM pairs in the either C3S-Energy or ECEM were replaced (or additional GCM-RCM simulations added), then there is a risk that the multi-model average might be quite different. This risk is further exacerbated by recalling the ad-hoc nature of the climate simulations considered: for example, although there are 11 different GCM-RCM pairs available in C3S-Energy, only 10 can be used (because the global climate model run for C3S_ECE_HIR is unavailable) and this corresponds to just 6 different GCMs (one of which provides an initial condition ensemble of size 2), paired with 8 different RCMs.

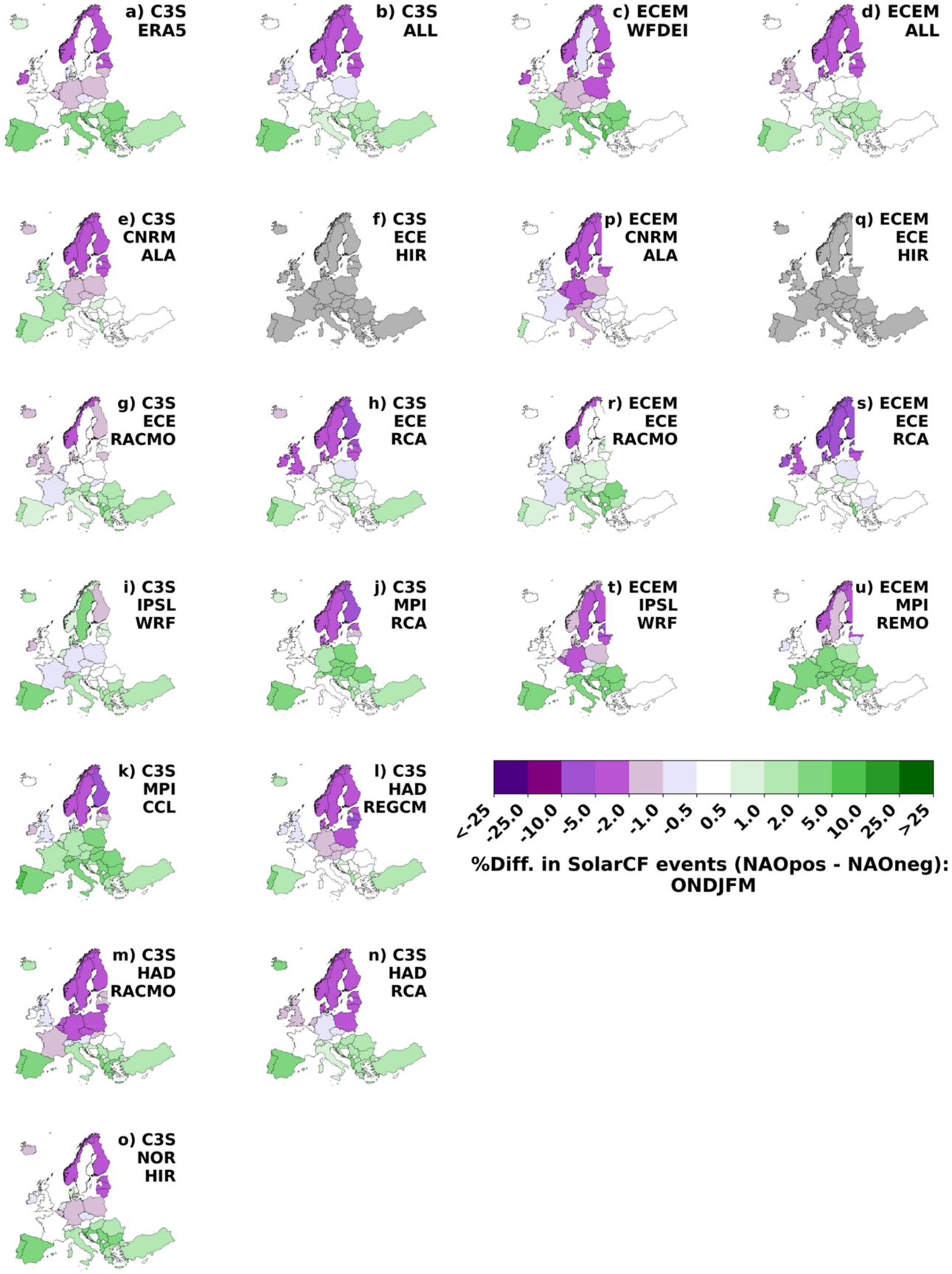

FIGURE 8 | As Figure 7 but for solar CF.

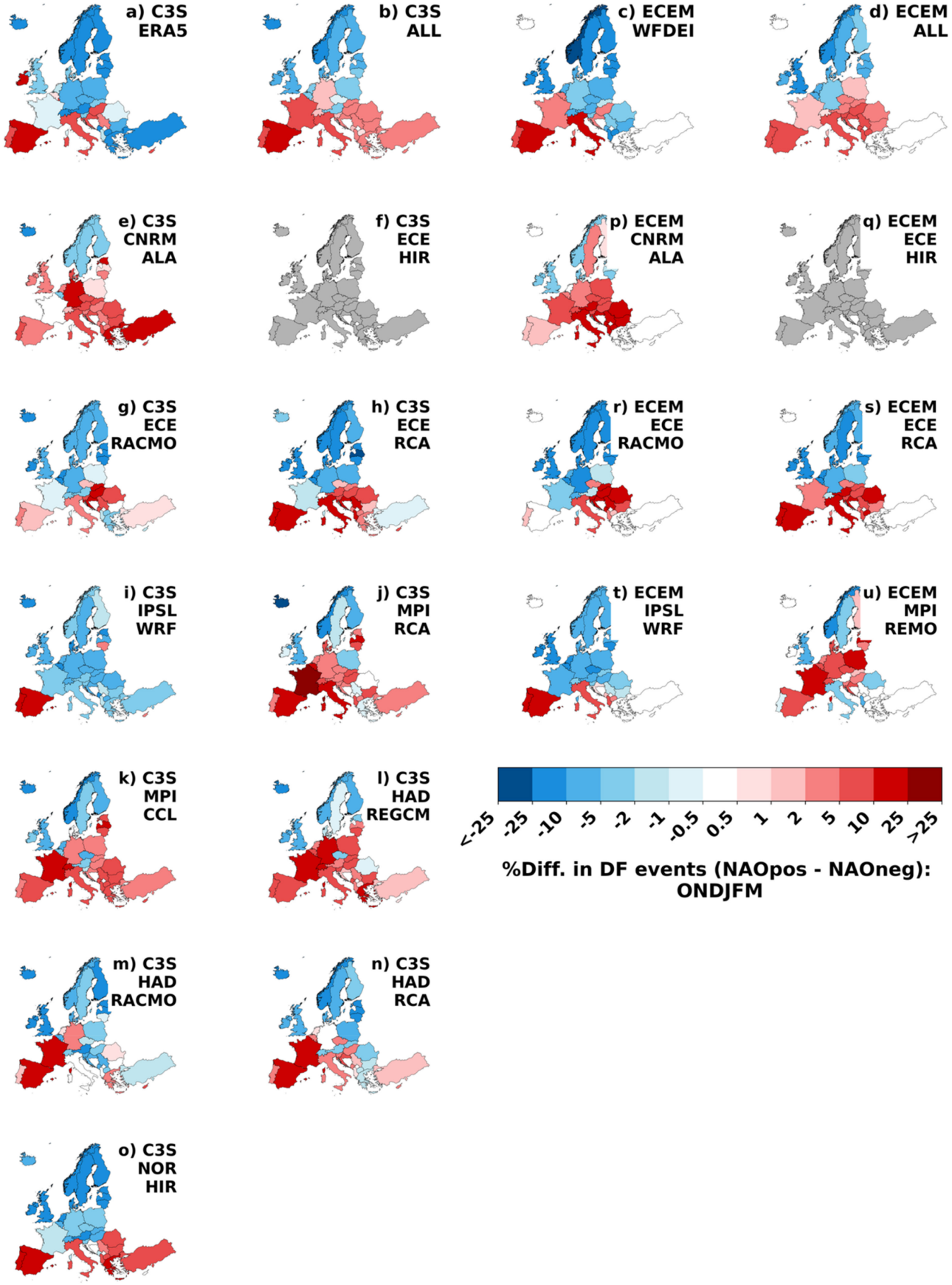

FIGURE 9 | As Figure 7 but for DF events.

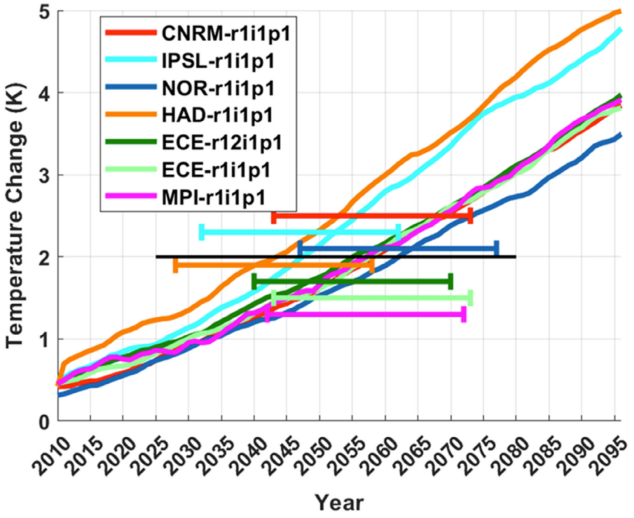

FIGURE 10 | The global mean change in surface 2m air temperature relative to the historical baseline (1980–2010). The solid black line indicates the +2°C threshold. The coloured horizontal bars represent the selected future 30-year time periods for each model (for each model, the period is centred on the year at which the 2°C level is passed) to be used for analysis. Please note that the vertical offset of the horizontal ranges is chosen for illustrative convenience only. See main text for discussion.

TABLE 2 | 30-year window centred on the year at which the 2°C global warming level is reached and associated shift in the 30-year mean ONDFJM NAO index in the parent GCMs for the C3S-Energy and ECEM databases.

Parent GCM	2°C warming period	NAO projection (ONDJFM)
ECE-r1i1p1	2043–2073	−0.308
HAD-r1i1p1	2029–2059	−0.163
CNRM-r1i1p1	2044–2074	−0.156
MPI-r1i1p1	2043–2073	−0.129
ECE-12i1p1	2041–2071	0.008
NOR-r1i1p1	2048–2078	0.138

Note: See main text for details.

Additional problems with multi-model averaging also exist. First, while taking an average over an ensemble—even one as small as those available from ECEM and C3S-Energy—can enhance signal-to-noise, it necessarily introduces smoothing and by construction limits the range of climate scenarios that result. Second, on a more fundamental level it is difficult to interpret ensemble-averages, as there is no physical justification for assuming the simulations they produce to be independent samples from an underlying 'true' population.

In order to address these issues, the individual model realisations are shown in Figure 12 for the C3S-Energy dataset models and Figure 13 for ECEM. An obvious feature is that two GCM-RCM combinations have a markedly different response in solar CF compared to all the others (ECEM_CNRM_ALA/C3S_CNRM_ALA and C3S_HAD_REGCM), emphasising the well-known uncertainties in representing cloud and solar in both global and regional climate models.

More broadly, a diverse range of individual responses is clearly visible, including marked changes (up to ~25% in some countries) though many fail to pass even a relatively modest statistical significance test (90% confidence) suggesting a significant role for internal variability in addition to inter-model differences (see, e.g., Gonzalez et al. 2019; Wohland 2022). It is noted, however, that the differences between the individual model outputs do not appear to be readily explainable as large-scale circulation changes that create shifts towards different NAO-like states (c.f., Ravestein et al. 2018): that is, models that project onto similar 30-year mean ONDJFM NAO anomalies are associated with qualitatively different outcomes in terms of surface energy climate (e.g., C3S_CNRM_ALA and C3S_HAD_RCA have almost identical projected changes in the NAO but markedly different changes in wind CF, solar CF and DF characteristics—compare Figure 12 Panels a1–a4 with Panels j1–j4). Indeed, even simulations drawn from identical parent GCM data (i.e., a single realisation of HadGEM2-ES) can have markedly different projected changes (compare Figure 12 Panels i1–4 with Panels j1–j4). As expected, however, when the same GCM-RCM pairs are compared in ECEM and C3S-Energy (e.g., C3S_CNRM_ALA is compared to ECEM_CNRM_ALA; Figure 12 Panels a1–4 with Figure 13 Panels a1–4), the responses are rather similar (in this case generally a decrease in DF). This indicates again that the uncertainty from the selection and extent of the climate model ensemble (i.e., the number of GCM and RCMs used) dominates over the uncertainty associated with the bias adjustment and conversion to energy steps.

While identifying a full range of responses from the ensemble is a helpful step in revealing a wide range of possible futures (here 15 in total: 10 from C3S-Energy and 5 from ECEM as opposed to a single 'multi-model average'), it is perhaps challenging for users in the energy industry to understand and interpret their consequences in a physically meaningful way. Following the 'Storyline' concept (discussed in Shepherd 2019), a qualitative grouping of these 15 different scenarios has therefore been developed. This grouping aims to recognise the broad character of the inter-model differences in future climate while clumping similar simulations together to reduce the overall number. As the responses for any given individual model were qualitatively similar in ECEM and C3S-Energy (i.e., the climate model uncertainty dominated over that produced by the bias adjustment and conversion), the two are merged into a single grand ensemble. Although this leads to different storylines being associated with very different numbers of model realisations, it is noted that the model simulations and datasets should not be considered independent or identically distributed (e.g., the EC-EARTH model contributes 4 realisations of the 15 whereas NORESM1 only 1). It is therefore inappropriate at this stage to consider some storylines as more likely than others. However, as climate change proceeds, assessments of changes in patterns of DF changes may be able to provide growing confidence about which of these storylines are more likely to be realised at 2°C warming. Additional detailed investigation of historical model runs may also enable

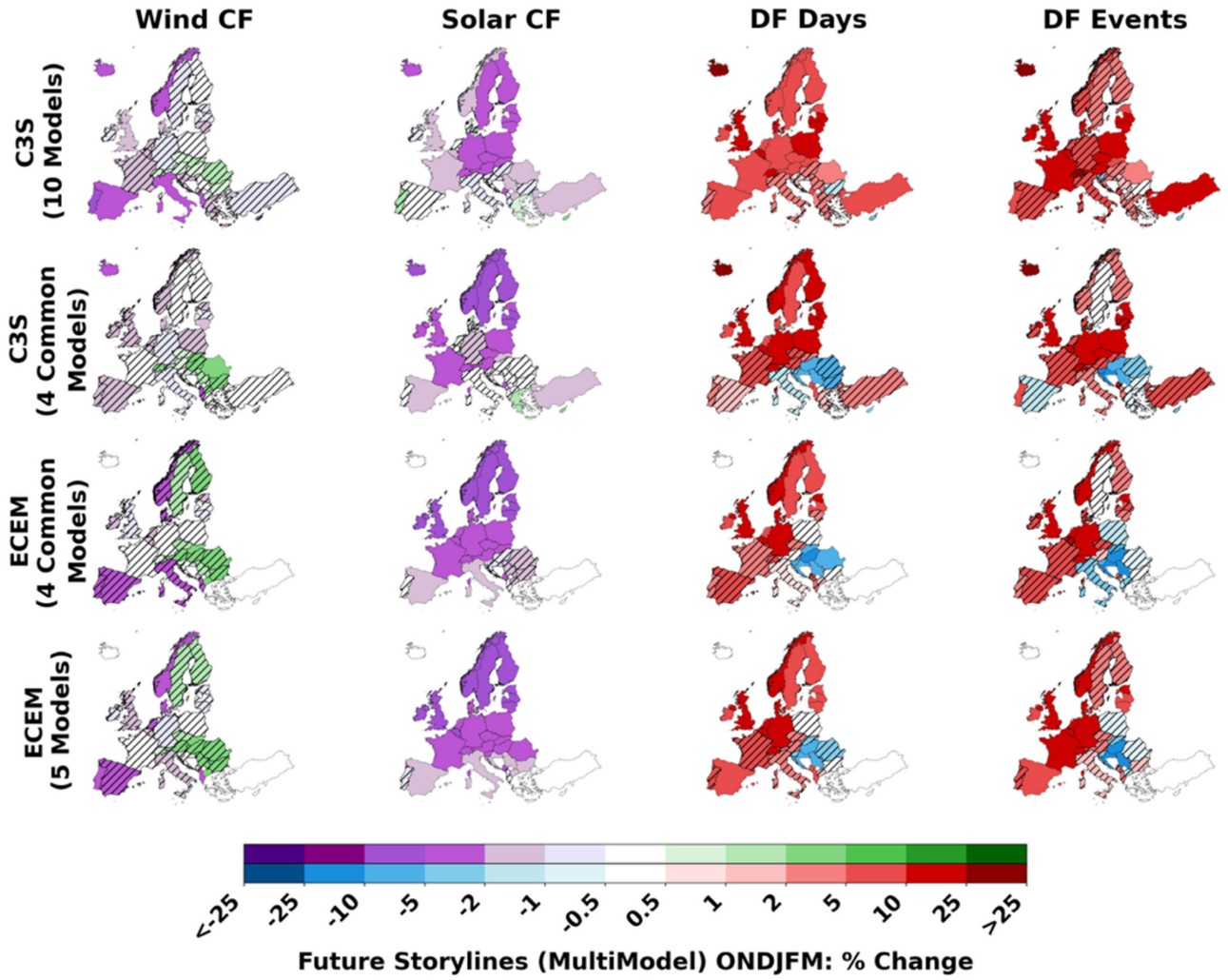

FIGURE 11 | Projected percentage change in extended winter (ONDFJM) wind capacity factor (1st column: a1, b1, c1, d1), solar capacity factor (2nd column: a2, b2, c2, d2), DF days (3rd column: a3, b3, c3, d3) and number of DF events (4th column: a4, b4, c4, d4) under a 2°C warming scenario relative to 1980–2010 in C3S projections. Top row (a1–a4): multi-model average over ten C3S models (all C3S models except C3S_ECE_HIR). 2nd row (b1–b4): multi-model average over four C3S models common to both C3S-Energy and ECEM (C3S_CNRM_ALA, C3S_ECE_RCA, C3S_ECE_RACMO, C3S_IPSL_WRF). 3rd row (c1–c4): multi-model average over four ECEM models (MPI, CNRM, IPSL, ECEarth) common to both C3S-Energy and ECEM (ECEM_CNRM_ALA, ECEM_ECE_RCA, ECEM_ECE_RACMO, ECEM_IPSL_WRF). 4th row (d1–d4): multi-model average over five ECEM models (all ECEM models except ECEM_ECE_HIR). Hatching denotes areas with non-significant changes based on 90% confidence from the Wilcoxon signed-rank test. Note data from C3S_ECE_HIR and ECEM_ECE_HIR is not included here as it was not possible to identify a 2°C warming scenario from the parent GCM simulation.

some storylines to be ruled out, as models diverge from historical trends or are shown to exhibit implausible physical responses.

The five resulting storylines are presented in Figure 14 and can be described as follows:

- Storyline 1 (Figure 14a1–a4; C3S_HAD_RCA): Wind CF and solar CF decrease over most of the domain. DF increases over most of the domain.
- Storyline 2 (Figure 14b1; C3S_NOR_HIR, C3S_IPSL_WRF, ECEM_IPSL_WRF): Wind CF increases in the north and decreases in the south. Solar CF decreases over most of the domain. DF increases over most of the domain.
- Storyline 3 (Figure 14c1–c4; C3S_MPI_RCA, C3S_ECE_RCA, C3S_ECE_RACMO, C3S_HAD_RACMO, C3S_MPI_CCL, ECEM_MPI_REMO, ECEM_ECE_RCA, ECEM_ECE_RACMO): Wind CF increases in the south/east and decreases in the north/west. Solar CF decreases over most of the domain. DF increases in the north/west with a slight decrease in the south/east.
- Storyline 4 (Figure 14d1–d4; C3S_HAD_REGCM). Wind CF decreases over most of the domain: Solar CF increases over the whole domain. DF decreases in the north and increases in the south.
- Storyline 5 (Figure 14e1–e4; C3S_CNRM_ALA, ECEM_CNRM_ALA): Wind CF increases in north/east and decreases in south/west. Solar CF increases in south and decreases in north. DF decreases over most of domain.

6 | Conclusions

The frequency of multi-day periods featuring low-wind and low-solar generation—often referred to as dunkelflaute (DF)—will be an increasingly important benchmark for the managers of European electrical grids as renewable generation's contribution to the system grows. Assessing the characteristics of DF and how they might change in a changing climate will be essential for robust design and operation of future power systems incorporating high levels of variable renewable generation. Recent years have seen the development of a number of climate services tailored to energy-system use, with the EU's COPERNICUS C3S-Energy and ECEM services being high-profile examples (both of which are based on the

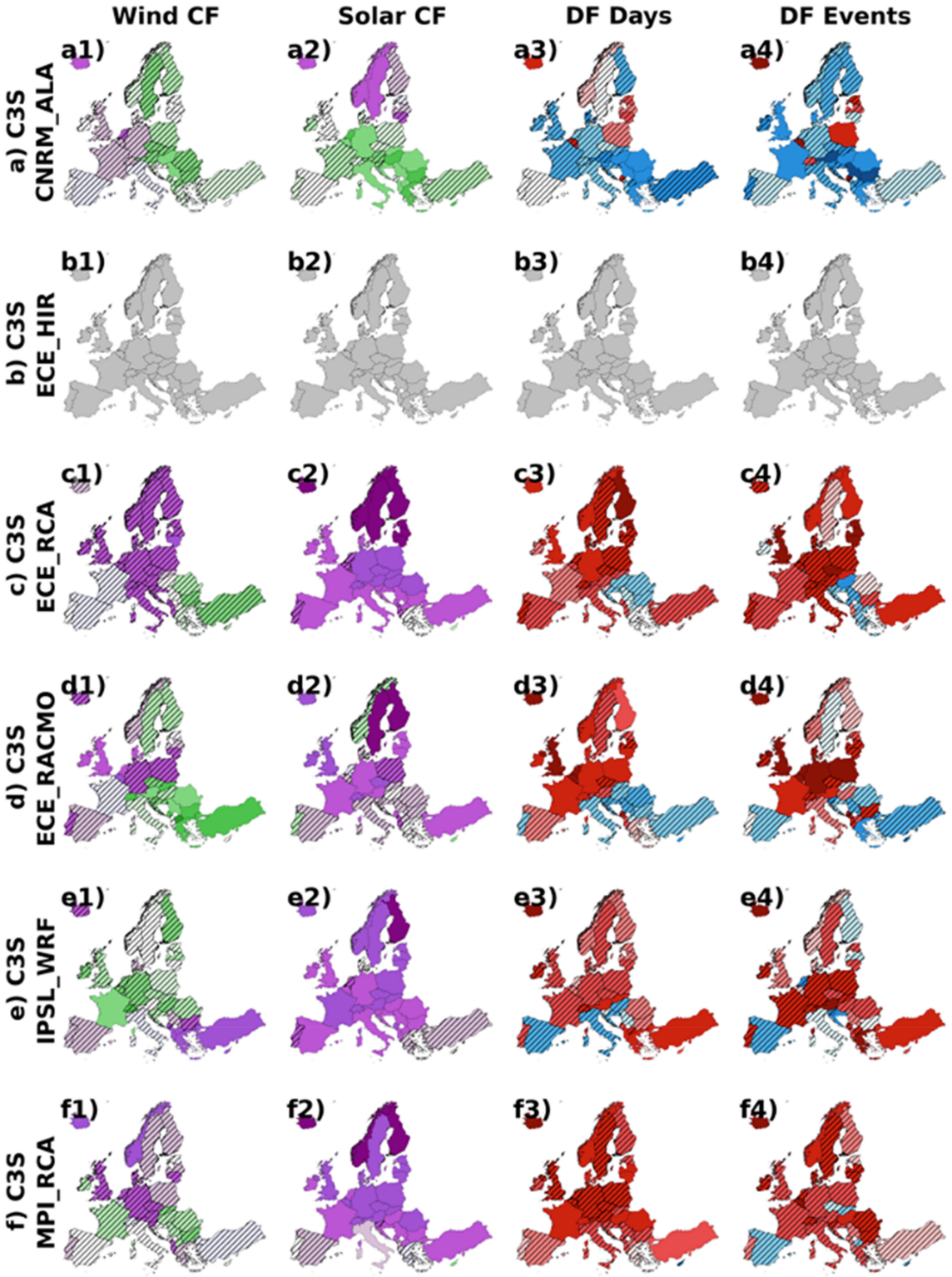

FIGURE 12 | As Figure 11, but showing individual model responses from the C3S-Energy dataset. Each row corresponds to a different model. Note C3S_ECE_HIR is greyed out as data for the corresponding parent GCM was not available to identify the 2°C warming level.

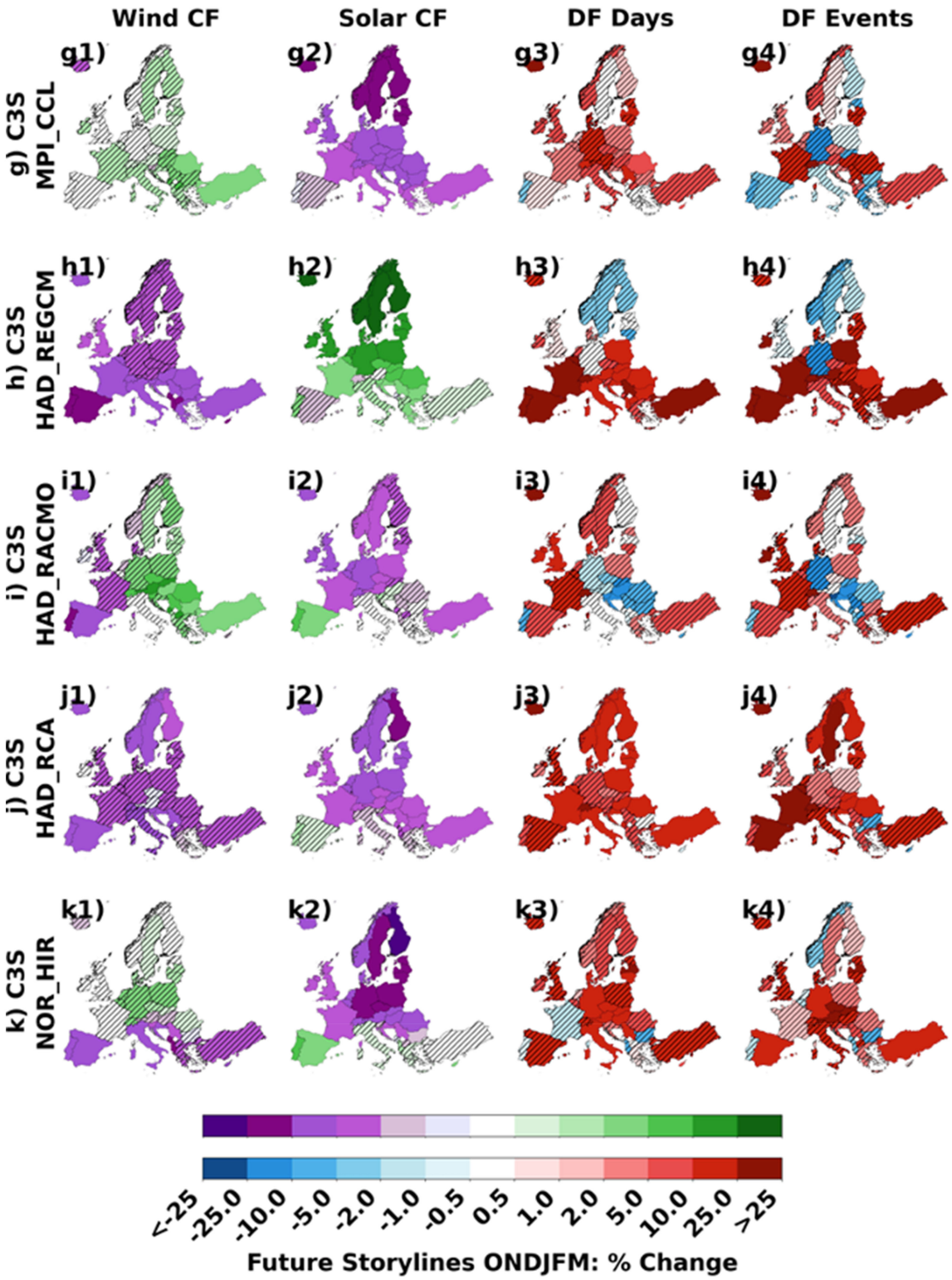

FIGURE 12 | (Continued)

EURO-CORDEX climate model dataset). This study assesses the suitability of these two services for characterising DF in the present and recent past, and for projecting changes in DF under a 2°C global warming scenario.

Overall, a reasonably coherent and self-consistent picture of DF behaviour over the historic period (1980–2010) emerges from both the C3S-Energy and ECEM dataset's. In each datasets reanalysis-based product, DF are most common in the extended winter (ONDJFM), the frequency of events is reasonably evenly distributed over Europe, and they respond to the dominant mode of North Atlantic—European atmospheric variability (the NAO) as one might expect (e.g., positive NAO periods are associated with windier but cloudier conditions in the north, with the 'wind' effect apparently dominating to produce fewer DF events). To a large extent, similar behaviours are found in

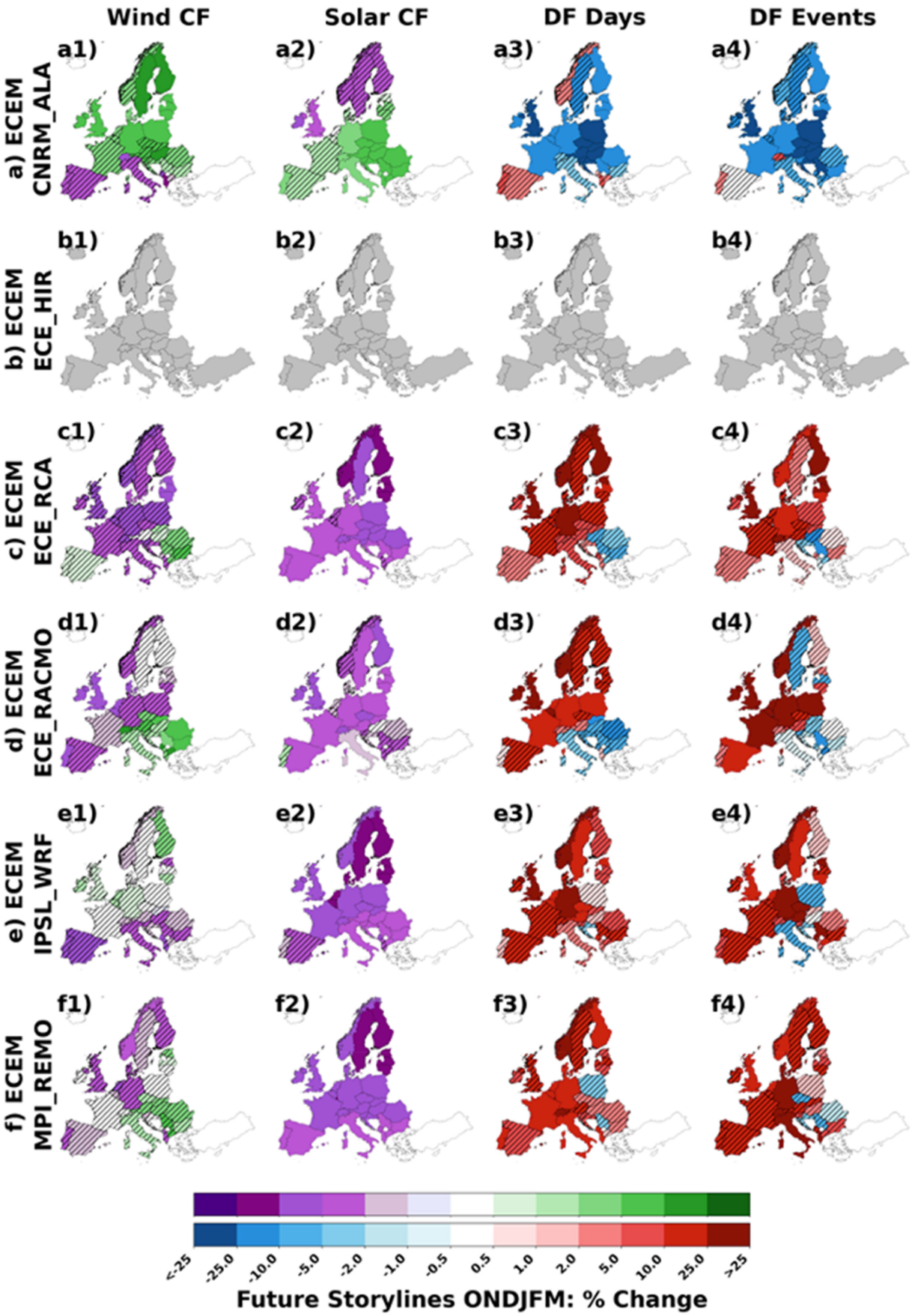

FIGURE 13 | As Figure 12, but showing individual model responses from the ECEM dataset. Note ECEM_ECE_HIR is greyed out as data for the corresponding parent GCM was not available to identify the 2°C warming level.

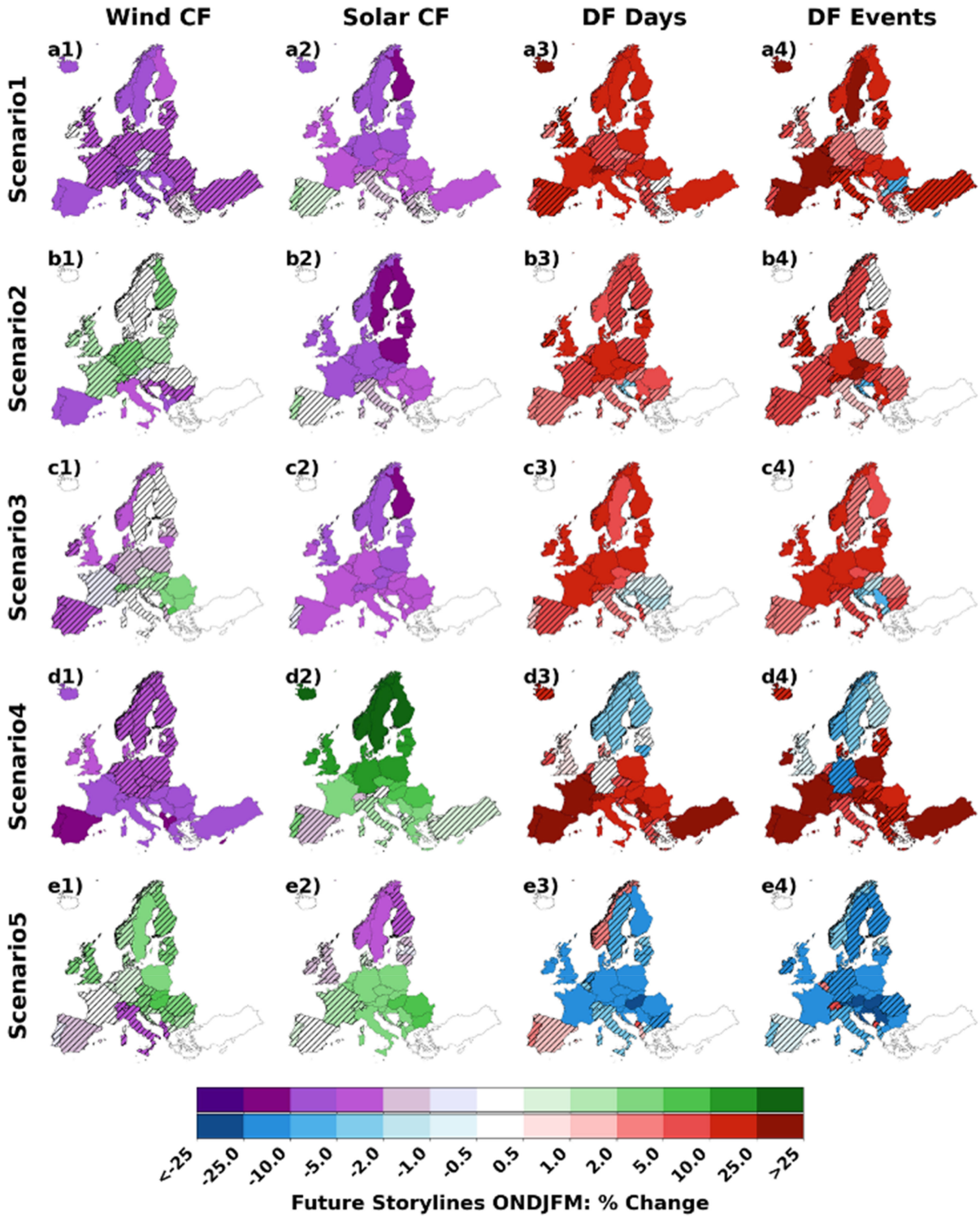

FIGURE 14 | Storyline groupings for the combined ECEM and C3S-Ener gy 2°C global warming scenarios. These groups are based on qualitatively assigning the individual model responses into consistent groups. Projected percentage change in extended winter (ONDFJM) wind capacity factor (1st column: a1, b1, c1, d1), solar capacity factor (2nd column: a2, b2, c2, d2), DF days (3rd column: a3, b3, c3, d3) and number of DF events (4th column: a4, b4, c4, d4) under a 2°C warming scenario relative to 1980–2010 in C3S projections. Each row corresponds to a different group of models. Top row (a1–a4): C3S_HAD_RCA. 2nd row (b1–4): C3S_NOR_HIR, C3S_IPSL_WRF, ECEM_IPSL_WRF. 3rd row: C3S_MPI_RCA, C3S_ECE_RCA, C3S_ECE_RACMO, C3S_HAD_RACMO, C3S_MPI_CCL, ECEM_MPI_REMO, ECEM_ECE_RCA, ECEM_ECE_RACMO. 4th row: C3S_HAD_REGCM. 5th row: C3S_CNRM_ALA, ECEM_CNRM_ALA. Hatching denotes areas with non-significant changes based on 90% confidence from the Wilcoxon signed-rank test. Note data from C3S_ECE_HIR and ECEM_ECE_HIR is not included here as it was not possible to identify a 2°C warming scenario from the parent GCM simulation.

the corresponding climate model simulations in each dataset, although it is important to note that the C3S-Energy climate models tend to produce rather more DF than their corresponding reanalysis (based on ERA5) and, when viewed at the level of individual countries rather than continental-scale patterns, there can be marked differences between individual model simulations.

This overall consistency only emerges, however, with careful and appropriate handling of the data. The 'raw' data from both C3S-Energy and ECEM contains noticeable differences both between the datasets (e.g., the reanalysis-based estimates of wind and solar capacity factors are markedly different in C3S-Energy and ECEM) and between the model and reanalysis data within each dataset (e.g., the wind and solar capacity factor data derived from the climate models in each dataset are not bias-adjusted to their associated reanalysis). As C3S-Energy is an operational product, this latter issue may have been corrected in more recent releases but, in the releases we are aware of, there is insufficient climate model data available for the historical period to facilitate a meaningful comparison. These issues are mitigated in this study by retrieving additional data (the ECEM_WFDEI dataset, see Section 2.2) and by using relative rather than absolute capacity factor thresholds to define DF events. However, the present study suggests that any services seeking to provide authoritative energy-climate products should, as a minimum, (a) provide sufficient time-window overlaps between observed-historical and model-simulated data (to facilitate validation), (b) ensure self-consistency between the observed and model-derived data and (c) provide a single reference source containing a clear description of the methods use and their validation. Prospective energy-sector users should also always ensure that they undertake a careful evaluation of the data before treating it at face value.

In terms of future projections of a 2°C global warming scenario, the multi-model mean response of C3S-Energy shows an increase in DF events ~5%–25% over much of the study domain. ECEM shows a similar pattern (and magnitude) except in that there is evidence for a slight decrease in DF in the south-east. Broadly speaking, this pattern is consistent with previous analysis of low-wind-low-solar conditions in the C3SE dataset (e.g., Figures 8 and 9) in Kapica et al. (2024) suggests increases in the mean wind-and-solar drought days over much of Europe, though with limited agreement between models.

Much of this difference, however, appears to be associated with the differences in the model ensembles considered (C3S-Energy has 10 realisations, ECEM 5) and there is much greater agreement when the multi-model average is restricted to only the models present in both datasets. The multi-model average therefore appears strongly determined by the collection of GCMs and RCM considered in each dataset, rather than differences in the post-processing used to create the energy data from the climate data. Though the present analysis has focussed primarily on DF, it is perhaps reasonable to expect similar sensitivity in projections of wind- and solar-capacity factors individually (as noted previously in Bloomfield, Brayshaw, Troccoli, et al. 2021).

As the ensemble of GCMs and RCMs is largely one of opportunity (i.e., constrained by the modelling groups participating in the EURO-CORDEX programme and subselected following the method of Bartók et al. 2019), reliance on the multi-model mean as a unique 'best prediction of the future' is not always appropriate as it may miss a wide range of uncertainty associated with alternative future pathways. This risk is clearly evidenced by the diverse individual responses, at least some of which show opposing responses (i.e., widespread decreases in DF rather than increases). While handling the full set of model outcomes may be rather intractable for energy-sector users of a climate service (i.e., understanding the impact of all 15 GCM-RCM combinations from ECEM and C3S-Energy together), a plausible route forward using just five plausible 'storylines' of future changes in DF and wind/solar capacity factors is proposed.

It is concluded that, subject to the need for appropriate and careful handling, the ECEM and C3S-Energy datasets provide a good starting point for exploring future climate impacts on the European energy system. Nevertheless, it is also clear that a much deeper exploration of a more comprehensive set of climate simulations is needed in order to robustly understand and predict the impact of future climate on energy. In particular, the ECEM and C3S-Energy are insufficiently comprehensive to isolate and understand the uncertainties arising from (a) individual model errors (GCM and RCM), and (b) internal variability, thereby limiting the confidence which can be ascribed to their projections. These difficulties are exacerbated by the well-known uncertainties associated with climate model representations of near-surface climate for wind and solar (especially the uncertainty associated with representing cloud processes).

Opportunities to gather much more comprehensive climate datasets for energy should therefore be actively pursued, for example, via the CMIP7 'Energy System Impacts' data request (Ruane et al. 2025) and individual single-model large ensembles (e.g., van der Wiel, Bloomfield, et al. 2019). A particular focus from this should be the representation of cloud processes (in relation to solar generation) and boundary-layer wind speed change (in relation to wind power), where additional simulations should be supported by deeper process-based understanding of the causes of change. Furthermore, none of the climate simulations considered here represent the impact of so-called 'tipping point' scenarios (such as abrupt weakening of the Atlantic Meridional Overturning Circulation see, e.g., Meccia et al. 2025 and Brayshaw et al. 2009) or the consequences of geoengineering solutions (Harding et al. 2024). Many of these plausible future scenarios may lead to European climate futures that differ substantially from the 'mainstream' projections and therefore warrant further investigation given the socio-economic importance and scale of transformation currently occurring in the energy sector.

Author Contributions

Laura West Fischer: investigation, project administration, supervision, writing – review and editing. **Daniel B. Kirk-Davidoff:** investigation, project administration, supervision, writing – review and editing. **Salim Poovadiyil:** data curation, formal analysis,

investigation, software, validation, visualization, writing – review and editing. **David J. Brayshaw:** conceptualization, formal analysis, methodology, investigation, validation, supervision, funding acquisition, visualization, project administration, writing – original draft, writing – review and editing.

Funding

This project was funded by Electric Power Research Institute (EPRI), agreement number 10016402.

Conflicts of Interest

D.J.B. declares his prior involvement as a member of the project team responsible for developing the COPERNICUS ECEM climate service demonstrator (grant number: 2015/C3S_441_Lot2).

Data Availability Statement

The data that support the findings of this study are openly available from the ECEM website (https://ecem.tealtool.earth) and the Copernicus Climate Data Store (CDS, https://cds.climate.copernicus.eu).

References

Bacer, S., F. Jomaa, J. Beaumet, et al. 2021. "Impact of Climate Change on Wintertime European Atmospheric Blocking." *Weather and Climate Dynamics Discussions* 2021: 1–21.

Bartók, B., I. Tobin, R. Vautard, et al. 2019. "A Climate Projection Dataset Tailored for the European Energy Sector." *Climate Services* 16: 100138.

Bloomfield, H. C. 2025. "Reasonable Worst-Case Stress-Test Scenarios for the UK Energy Sector in the Context of the Changing Climate: A Synthesis Report Developed for the UK Climate Change Committee." Technical report. https://www.theccc.org.uk/wp-content/uploads/2025/02/Reasonable-worst-case-stress-test-scenarios-for-the-UK-energy-sector-in-the-context-of-the-changing-climate-Bloomfield.pdf.

Bloomfield, H. C., D. J. Brayshaw, and A. J. Charlton-Perez. 2020. "Characterizing the Winter Meteorological Drivers of the European Electricity System Using Targeted Circulation Types." *Meteorological Applications* 27, no. 1: e1858.

Bloomfield, H. C., D. J. Brayshaw, P. L. Gonzalez, and A. Charlton-Perez. 2021. "Pattern-Based Conditioning Enhances Sub-Seasonal Prediction Skill of European National Energy Variables." *Meteorological Applications* 28, no. 4: e2018.

Bloomfield, H. C., D. J. Brayshaw, P. L. M. Gonzalez, and A. Charlton-Perez. 2021. "Sub-Seasonal Forecasts of Demand, Wind Power and Solar Power Generation for 28 European Countries." *Earth System Science Data* 13, no. 5: 2259–2274.

Bloomfield, H. C., D. J. Brayshaw, A. Troccoli, et al. 2021. "Quantifying the Sensitivity of European Power Systems to Energy Scenarios and Climate Change Projections." *Renewable Energy* 164: 1062–1075.

Brayshaw, D. J., T. Woollings, and M. Vellinga. 2009. "Tropical and Extratropical Responses of the North Atlantic Atmospheric Circulation to a Sustained Weakening of the MOC." *Journal of Climate* 22, no. 11: 3146–3155.

Bundesministerium für Wirtschaft und Energie. 2025. "Time Series for the Development of Renewable Energy Sources in Germany (February 2025)." Federal Ministry for Economic Affairs and Climate Action. https://www.bundeswirtschaftsministerium.de/Redaktion/DE/Downloads/Energie/zeitreihen-zur-entwicklung-der-erneuerbaren-energien-in-deutschland-1990-2024-en.pdf?__blob=publicationFile&v=10.

Cannon, D. J., D. J. Brayshaw, J. Methven, P. J. Coker, and D. Lenaghan. 2015. "Using Reanalysis Data to Quantify Extreme Wind Power Generation Statistics: A 33 Year Case Study in Great Britain." *Renewable Energy* 75: 767–778.

Copernicus. 2018. "CMIP5 Monthly Data on Single Levels." https://cds.climate.copernicus.eu/datasets/projections-cmip5-monthly-single-levels.

Copernicus. 2024. *Climate and Energy Related Variables From the Pan-European Climate Database Derived From Reanalysis and Climate Projections*. Dataset and associated documentation. https://cds.climate.copernicus.eu/datasets/sis-energy-pecd.

Copernicus. 2025. "Services for the Energy Sector." https://climate.copernicus.eu/operational-service-energy-sector.

Davini, P., C. Cagnazzo, R. Neale, and J. Tribbia. 2012. "Coupling Between Greenland Blocking and the North Atlantic Oscillation Pattern." *Geophysical Research Letters* 39, no. 14: L14701.

Davini, P., and F. d'Andrea. 2020. "From CMIP3 to CMIP6: Northern Hemisphere Atmospheric Blocking Simulation in Present and Future Climate." *Journal of Climate* 33, no. 23: 10021–10038.

Dawkins, L. C., I. Rushby, A. Dobbie, E. Wallace, and T. Butcher. 2020. "Characterising Adverse Weather for the UK Electricity System." Including Addendum for Surplus Generation Events. United Kingdom Meteorological Office.

Drew, D. R., D. J. Cannon, D. J. Brayshaw, J. F. Barlow, and P. J. Coker. 2015. "The Impact of Future Offshore Wind Farms on Wind Power Generation in Great Britain." *Resources* 4, no. 1: 155–171.

Drücke, J., M. Borsche, P. James, et al. 2021. "Climatological Analysis of Solar and Wind Energy in Germany Using the Grosswetterlagen Classification." *Renewable Energy* 164: 1254–1266.

Dubus, L., D. J. Brayshaw, D. Huertas-Hernando, et al. 2022. "Towards a Future-Proof Climate Database for European Energy System Studies." *Environmental Research Letters* 17, no. 12: 121001.

Dubus, L., Y. M. Saint-Drenan, A. Troccoli, et al. 2023. "C3S Energy: A Climate Service for the Provision of Power Supply and Demand Indicators for Europe Based on the ERA5 Reanalysis and ENTSO-E Data." *Meteorological Applications* 30, no. 5: e2145.

Dunn-Sigouin, E., and S. W. Son. 2013. "Northern Hemisphere Blocking Frequency and Duration in the CMIP5 Models." *Journal of Geophysical Research: Atmospheres* 118, no. 3: 1179–1188.

ECEM. 2025. "The European Climatic Energy Mixes (ECEM) Demonstrator." Website and Dataset. https://ecem.tealtool.earth.

Ember. 2025. "European Electricity Review 2025." https://ember-energy.org/latest-insights/european-electricity-review-2025/.

ENTSO. 2020. "Mid-Term Adequacy Forecast: Executive Summary." ENTSO Report. https://eepublicdownloads.entsoe.eu/clean-documents/sdc-documents/MAF/2020/MAF_2020_Executive_Summary.pdf.

Feldstein, S. B. 2003. "The Dynamics of NAO Teleconnection Pattern Growth and Decay." *Quarterly Journal of the Royal Meteorological Society* 129, no. 589: 901–924.

Gonzalez Aparicio, I., T. Huld, F. Careri, F. Monforti Ferrario, and A. Zucker. 2017. "Solar Hourly Generation Time Series at Country, NUTS 1, NUTS 2 Level and Bidding Zones." European Commission, Joint Research Centre (JRC). http://data.europa.eu/89h/jrc-emhires-solar-generation-time-series.

Gonzalez, P. L., D. J. Brayshaw, and G. Zappa. 2019. "The Contribution of North Atlantic Atmospheric Circulation Shifts to Future Wind Speed Projections for Wind Power Over Europe." *Climate Dynamics* 53, no. 7: 4095–4113.

Harding, A., G. A. Vecchi, W. Yang, and D. W. Keith. 2024. "Impact of Solar Geoengineering on Temperature-Attributable Mortality."

Proceedings of the National Academy of Sciences 121, no. 52: e2401801121.

Hersbach, H., B. Bell, P. Berrisford, et al. 2020. "The ERA5 Global Reanalysis." *Quarterly Journal of the Royal Meteorological Society* 146, no. 730: 1999–2049.

IPCC. 2023. *Summary for Policymakers. In: Climate Change 2023: Synthesis Report*, edited by H. Lee and J. Romero, 1–34. Contribution of Working Groups I, II and III to the Sixth Assessment Report of the Intergovernmental Panel on Climate Change.

Jones, P. D., C. Harpham, A. Troccoli, et al. 2017. "Using ERA-Interim Reanalysis for Creating Datasets of Energy-Relevant Climate Variables." *Earth System Science Data* 9, no. 2: 471–495.

Kapica, J., J. Jurasz, F. A. Canales, et al. 2024. "The Potential Impact of Climate Change on European Renewable Energy Droughts." *Renewable and Sustainable Energy Reviews* 189: 114011.

Kaspar, F., M. Borsche, U. Pfeifroth, J. Trentmann, J. Drücke, and P. Becker. 2019. "A Climatological Assessment of Balancing Effects and Shortfall Risks of Photovoltaics and Wind Energy in Germany and Europe." *Advances in Science and Research* 16: 119–128.

Kies, A., K. Chattopadhyay, L. von Bremen, E. Lorenz, and D. Heinemann. 2016. "Restore 2050: Simulation of Renewable Feed-In for Power System Studies." Rep, Tech. Rep Tech.

Kies, A., B. U. Schyska, M. Bilousova, O. El Sayed, J. Jurasz, and H. Stoecker. 2021. "Critical Review of Renewable Generation Datasets and Their Implications for European Power System Models." *Renewable and Sustainable Energy Reviews* 152: 111614.

Kittel, M., and W. P. Schill. 2024. "Measuring the Dunkelflaute: How (Not) to Analyze Variable Renewable Energy Shortage." *Environmental Research: Energy* 1, no. 3: 035007.

Leahy, P. G., and E. J. McKeogh. 2013. "Persistence of Low Wind Speed Conditions and Implications for Wind Power Variability." *Wind Energy* 16, no. 4: 575–586.

Li, B., S. Basu, S. J. Watson, and H. W. Russchenberg. 2021. "A Brief Climatology of Dunkelflaute Events Over and Surrounding the North and Baltic Sea Areas." *Energies* 14, no. 20: 6508.

Lledó, L., J. Ramon, A. Soret, and F. J. Doblas-Reyes. 2022. "Seasonal Prediction of Renewable Energy Generation in Europe Based on Four Teleconnection Indices." *Renewable Energy* 186: 420–430.

Masato, G., T. Woollings, and B. J. Hoskins. 2014. "Structure and Impact of Atmospheric Blocking Over the Euro-Atlantic Region in Present-Day and Future Simulations." *Geophysical Research Letters* 41, no. 3: 1051–1058.

Matsueda, M., and H. Endo. 2017. "The Robustness of Future Changes in Northern Hemisphere Blocking: A Large Ensemble Projection With Multiple Sea Surface Temperature Patterns." *Geophysical Research Letters* 44, no. 10: 5158–5166.

Meccia, V. L., C. Simolo, K. Bellomo, and S. Corti. 2025. "The Impact of a Weakened AMOC on European Heatwaves." *Environmental Research Letters* 20, no. 2: 024005.

Mockert, F., C. M. Grams, T. Brown, and F. Neumann. 2023. "Meteorological Conditions During Periods of Low Wind Speed and Insolation in Germany: The Role of Weather Regimes." *Meteorological Applications* 30, no. 4: e214.

Mokhov, I. I., A. V. Timazhev, and A. R. Lupo. 2014. "Changes in Atmospheric Blocking Characteristics Within Euro-Atlantic Region and Northern Hemisphere as a Whole in the 21st Century From Model Simulations Using RCP Anthropogenic Scenarios." *Global and Planetary Change* 122: 265–270.

Moraes, L., Jr., C. Bussar, P. Stöcker, K. Jacqué, M. Chang, and D. U. Sauer. 2018. "Comparison of Long-Term Wind and Photovoltaic Power Capacity Factor Datasets With Open-License." *Applied Energy* 225: 209–220.

Novacheck, J., J. Sharp, M. Schwarz, et al. 2021. *The Evolving Role of Extreme Weather Events in the U.S.* Power System with High Levels of Variable Renewable Energy. Technical Report. NREL. https://doi.org/10.2172/1837959.

Ohlendorf, N., and W. P. Schill. 2020. "Frequency and Duration of Low-Wind-Power Events in Germany." *Environmental Research Letters* 15, no. 8: 084045.

Otero, N., O. Martius, S. Allen, H. Bloomfield, and B. Schaefli. 2022. "Characterizing Renewable Energy Compound Events Across Europe Using a Logistic Regression-Based Approach." *Meteorological Applications* 29, no. 5: e2089.

Patlakas, P., G. Galanis, D. Diamantis, and G. Kallos. 2017. "Low Wind Speed Events: Persistence and Frequency." *Wind Energy* 20, no. 6: 1033–1047.

Pozo-Vázquez, D., J. Tovar-Pescador, S. R. Gámiz-Fortis, M. J. Esteban-Parra, and Y. Castro-Díez. 2004. "NAO and Solar Radiation Variability in the European North Atlantic Region." *Geophysical Research Letters* 31, no. 5: L05201.

Ravestein, P., G. Van der Schrier, R. Haarsma, R. Scheele, and M. Van den Broek. 2018. "Vulnerability of European Intermittent Renewable Energy Supply to Climate Change and Climate Variability." *Renewable and Sustainable Energy Reviews* 97: 497–508.

Ruane, A. C., C. L. Pascoe, C. Teichmann, et al. 2025. "CMIP7 Data Request: Impacts and Adaptation Priorities and Opportunities." *Geoscientific Model Development* 18, no. 23: 9497–9540.

Schiemann, R., P. Athanasiadis, D. Barriopedro, et al. 2020. "Northern Hemisphere Blocking Simulation in Current Climate Models: Evaluating Progress From the Climate Model Intercomparison Project Phase 5 to 6 and Sensitivity to Resolution." *Weather and Climate Dynamics* 1, no. 1: 277–292.

Shepherd, T. G. 2019. "Storyline Approach to the Construction of Regional Climate Change Information." *Proceedings of the Royal Society A* 475, no. 2225: 20190013.

Smith, D. M., A. A. Scaife, R. Eade, et al. 2020. "North Atlantic Climate Far More Predictable Than Models Imply." *Nature* 583, no. 7818: 796–800.

Staffell, I., and S. Pfenninger. 2016. "Using Bias-Corrected Reanalysis to Simulate Current and Future Wind Power Output." *Energy* 114: 1224–1239.

Sung, M. K., G. H. Lim, J. S. Kug, and S. I. An. 2011. "A Linkage Between the North Atlantic Oscillation and Its Downstream Development due to the Existence of a Blocking Ridge." *Journal of Geophysical Research: Atmospheres* 116, no. D11: D11107.

Troccoli, A., C. Goodess, P. Jones, et al. 2018. "Creating a Proof-Of-Concept Climate Service to Assess Future Renewable Energy Mixes in Europe: An Overview of the C3S ECEM Project." *Advances in Science and Research* 15: 191–205.

Trocolli, A., T. Fuchs, and R. Boscolo. 2024. "Climate and Energy Indicators for Europe Datasets: Technical Description of Methodologies Followed in the Development of Each Product." Technical Documents. https://confluence.ecmwf.int/display/CKB/Climate+and+energy+indicators+for+Europe+datasets%3A+Technical+description+of+methodologies+followed+in+the+development+of+each+product.

van der Wiel, K., H. C. Bloomfield, R. W. Lee, et al. 2019. "The Influence of Weather Regimes on European Renewable Energy Production and Demand." *Environmental Research Letters* 14, no. 9: 094010.

van der Wiel, K., L. P. Stoop, B. R. H. Van Zuijlen, R. Blackport, M. A. Van den Broek, and F. M. Selten. 2019. "Meteorological Conditions Leading to Extreme Low Variable Renewable Energy Production and Extreme High Energy Shortfall." *Renewable and Sustainable Energy Reviews* 111: 261–275.

Weedon, G. P., G. Balsamo, N. Bellouin, S. Gomes, M. J. Best, and P. Viterbo. 2014. "The WFDEI Meteorological Forcing Data Set: WATCH Forcing Data Methodology Applied to ERA-Interim Reanalysis Data." *Water Resources Research* 50, no. 9: 7505–7514.

Wilczak, J. M., D. B. Kirk-Davidoff, H. Bloomfield, C. Bracken, and J. Sharp. 2025. "Wind and Solar Energy Droughts: Potential Impacts on Energy System Dynamics and Research Needs." *Journal of Renewable and Sustainable Energy* 17, no. 2: 022301.

Wohland, J. 2022. "Process-Based Climate Change Assessment for European Winds Using EURO-CORDEX and Global Models." *Environmental Research Letters* 17, no. 12: 124047.

Woollings, T., D. Barriopedro, J. Methven, et al. 2018. "Blocking and Its Response to Climate Change." *Current Climate Change Reports* 4, no. 3: 287–300.

Yao, Y., and D. Luo. 2015. "Do European Blocking Events Precede North Atlantic Oscillation Events?" *Advances in Atmospheric Sciences* 32, no. 8: 1106–1118.

Supporting Information

Additional supporting information can be found online in the Supporting Information section. **Table S1:** List of CMIP5/CORDEX models used in this publication. **Table S2:** Climatological annual rate of low wind, solar and low-wind-low-solar CF in the ECEM and C3S-Energy reanalyses (1980–2010). 'Low' is defined as daily-mean CF <0.2. **Figure S1:** Comparison of mean annual cycle in wind CF from ECEM and C3S-Energy datasets (1980–2010) for Germany: (a) Bulgaria, (b) France, (c) Germany, (d) Spain, (e) Sweden and (f) the UK. Black lines relate to reanalysis based estimates, coloured lines to climate-model based estimates. Solid lines related to C3S-Energy, dashed lines to ECEM. **Figure S2:** As Figure S1 but for solar CF. **Figure S3:** Annual cycle of DF event (2 days or more) frequency for the historical period (1980–2010) in reanalysis datasets associated with ECEM and C3S-Energy for Germany: (a) Bulgaria, (b) France, (c) Germany, (d) Spain, (e) Sweden and (f) the UK. **Figure S4:** Errors in DF event rates by duration for all countries included for extended winter (ONDJFM)—compare Figure 6 from the main text. (a) and (b) 2–3 day events in C3S-Energy and ECEM respectively. (c) and (d) 4–5 day events. Errors are expressed as fractions of the country-specific DF event rate from the appropriate reanalysis (C3S-ERA5 or ECEM-WFDEI). **Figure S5:** Interannual variability of extended winter (ONDFJM) mean wind CF in each component of the ECEM and C3S-Energy datasets. Colours scale indicate one standard deviation. **Figure S6:** As Figure S5 but for solar CF. **Figure S7:** As Figure S5 but for DF days. **Figure S8:** As Figure S5 but for DF events.